



ARTICLE

Cell-cycle control of cell polarity in yeast

Kyle D. Moran^{1*} , Hui Kang^{1*}, Ana V. Araujo¹, Trevin R. Zyla¹, Koji Saito², Denis Tsygankov³ , and Daniel J. Lew¹ 

In many cells, morphogenetic events are coordinated with the cell cycle by cyclin-dependent kinases (CDKs). For example, many mammalian cells display extended morphologies during interphase but round up into more spherical shapes during mitosis (high CDK activity) and constrict a furrow during cytokinesis (low CDK activity). In the budding yeast *Saccharomyces cerevisiae*, bud formation reproducibly initiates near the G1/S transition and requires activation of CDKs at a point called “start” in G1. Previous work suggested that CDKs acted by controlling the ability of cells to polarize Cdc42, a conserved Rho-family GTPase that regulates cell polarity and the actin cytoskeleton in many systems. However, we report that yeast daughter cells can polarize Cdc42 before CDK activation at start. This polarization operates via a positive feedback loop mediated by the Cdc42 effector Ste20. We further identify a major and novel locus of CDK action downstream of Cdc42 polarization, affecting the ability of several other Cdc42 effectors to localize to the polarity site.

Introduction

In the yeast *Saccharomyces cerevisiae*, bud formation and cytokinesis are coordinated with progression through the cell cycle (Howell and Lew, 2012). Cell-cycle events are triggered by a regulatory network centered on cyclins and CDKs (Morgan, 1997). The major cell-cycle CDK is Cdc28, and it has long been clear that Cdc28 is required to promote bud emergence (Pringle and Hartwell, 1981). CDK activation by G1 cyclins promotes cell-cycle commitment at “start” in late G1, which is followed by actin polarization toward the presumptive bud site and assembly of a septin ring at that site (Howell and Lew, 2012). These cytoskeletal reorganizations are dependent on Cdc42, a highly conserved Rho-family GTPase that acts as the master regulator of cell polarity (Bi and Park, 2012). The mechanisms by which G1 cyclin/CDK activity regulates Cdc42-dependent polarization remain unclear.

Cdc42 itself becomes activated and concentrated at the presumptive bud site (Ziman et al., 1993; Gulli et al., 2000), and there has been considerable progress toward understanding how this occurs. Yeast cells are born with prelocalized transmembrane “landmark” proteins at the proximal and distal poles of the cell (Chant, 1999). Landmark proteins can localize Bud5, a guanine-nucleotide exchange factor (GEF) for the Ras-family GTPase Rsr1, presumably leading to the local activation of Rsr1. In turn, active Rsr1 can recruit Cdc24, the major GEF for Cdc42, from the cytoplasm to the cortex, promoting local activation of Cdc42 near the landmarks. Active Cdc42 then recruits more active Cdc42 through a positive feedback loop (Kozubowski et al.,

2008): Cdc42 binds effector p21-activated kinases (PAKs) Ste20 and Cla4, recruiting them from the cytoplasm to the nascent polarity site. PAKs bind and recruit the scaffold protein Bem1, which binds and recruits the GEF Cdc24. This results in enhanced Cdc42 activation wherever there is already some activated Cdc42, increasing the local concentrations of polarity proteins near the landmarks. In cells lacking Rsr1, clusters of Cdc42 appear at apparently random locations and are thought to result from positive feedback initiated by stochastic fluctuations in polarity protein concentrations (Howell et al., 2012).

Several studies indicated that G1 CDK activity is required to promote Cdc42 polarization: Cdc24 (Gulli et al., 2000), Cdc42 (Wedlich-Soldner et al., 2004), Bem1 (Butty et al., 2002), and the Cdc42 effectors Gic2 (Gulli et al., 2000) and Bni1 (Jaquenoud and Peter, 2000) were not detectably polarized in cells depleted of G1 cyclins, but became polarized after CDK activation. Moreover, bulk GTP-Cdc42 levels measured in synchronized cell populations increased at around the time of budding, consistent with cell-cycle control of Cdc42 (Atkins et al., 2013). On the other hand, the Bni1-interacting protein Spa2 (Padmashree and Surana, 2001) and a reporter for GTP-Cdc42 (Lee et al., 2015) were reported to polarize before CDK activation. It has been unclear why these different studies reached different conclusions.

Here, we revisited the timing of polarization in wild-type cells using time-lapse microscopy and multiple probes. We found that wild-type daughter cells polarized Cdc42 before CDK activation

¹Department of Pharmacology and Cancer Biology, Duke University, Durham, NC; ²Department of Biosciences, School of Science, Kitasato University, Kitasato, Sagami-hara, Kanagawa, Japan; ³Wallace H. Coulter Department of Biomedical Engineering, Georgia Institute of Technology and Emory University School of Medicine, Atlanta, GA.

*K.D. Moran and H. Kang contributed equally to this paper; Correspondence to Daniel J. Lew: daniel.lew@duke.edu; H. Kang's present address is Aptitude Medical Systems Inc., Santa Barbara, CA.

© 2018 Moran et al. This article is distributed under the terms of an Attribution–Noncommercial–Share Alike–No Mirror Sites license for the first six months after the publication date (see <http://www.rupress.org/terms/>). After six months it is available under a Creative Commons License (Attribution–Noncommercial–Share Alike 4.0 International license, as described at <https://creativecommons.org/licenses/by-nc-sa/4.0/>).

(prestart), whereas mother cells polarized after CDK activation. Prestart polarization required positive feedback via the Cdc42-Ste20-Bem1-Cdc24 feedback loop described above as well as Rsr1. However, prestart polarization did not engage the PAK Cla4 or other tested Cdc42 effectors, which remained unpolarized until after start. Our findings suggest the existence of an unexpected new pathway for the control of cell polarity by the cell cycle: CDK activity enables a subset of Cdc42 effectors to localize to sites with active Cdc42.

Results

Timing of polarization relative to cell-cycle start

We first examined the interval between start and polarization at the single-cell level. Cell-cycle commitment at start involves a positive feedback loop in which G1-CDK activity promotes transcription and hence accumulation of the G1 cyclins Cln1 and Cln2 (Skotheim et al., 2008). Transcription of CLNs and other CDK targets is repressed by the Rb analogue Whi5, and G1 CDK activity inactivates Whi5 and promotes its nuclear export (Costanzo et al., 2004; de Bruin et al., 2004). Passage through start occurs when 50% of the Whi5 has exited the nucleus (Doncic et al., 2011), and we used this criterion to mark start in our experiments. To assess the time of polarization, we used fluorescent probes for the GEF Cdc24, the scaffold protein Bem1, and Cdc42 itself (Materials and methods).

Wild-type diploid cells were presynchronized by hydroxyurea arrest-release, which reduces phototoxicity during subsequent imaging (Howell et al., 2012). Surprisingly, the timing of polarization differed significantly from cell to cell. In particular, daughter cells polarized before start, whereas mother cells polarized after start (Fig. 1). Comparable results were obtained for Bem1, Cdc24, and Cdc42 probes (Fig. 1, A–C).

We used unbiased image analysis tools (Lai et al., 2018) to quantify the nuclear export of Whi5 and the clustering of polarity probes (Materials and methods). Whi5 nuclear export was previously tracked by quantifying its nuclear concentration based on segmentation of nuclei using a second fluorescent probe (Doncic et al., 2011). We found that comparable results could be obtained using only the Whi5-GFP signal by tracking the coefficient of variation (CV) of the pixel intensities in individual cells (Fig. S1). When Whi5 was concentrated in the nucleus, there were bright pixels (nuclear) and dim pixels (cytoplasmic) in each cell, yielding a high CV. Upon Whi5 nuclear exit, all pixels displayed an intermediate intensity, yielding a low CV. We tracked the Whi5 CV over time, and smoothed the CV profile to call the time of start (50% decrease in Whi5 CV = 50% Whi5 nuclear exit; Fig. S1). Similarly, we used the pixel intensity CV for polarity probes to track the process of polarization. Unpolarized cells yielded a uniform pixel intensity and hence low CV, whereas polarized cells with bright pixels (polarity site) and dim pixels (elsewhere) yielded a higher CV. The smoothed CV profile was used to estimate the onset of polarization by calculating the maximum of the second derivative of the polarity probe CV with respect to time. For mother cells, this procedure picked a time of polarity onset one time point before the first polarized frame detectable by eye (Fig. S2). For daughter cells, many cells similarly displayed

an unambiguous time of polarity onset (e.g., Fig. 1 B), but some cells displayed a biphasic polarization with two onset times (e.g., Fig. 1 A). The earlier onset time corresponded with prestart initial polarization, whereas the later onset time corresponded to the poststart intensification of the polarity probe (Fig. 1 A). In what follows, we report the earlier onset time for such biphasic cells.

Determining the times of start and polarity onset allowed us to quantify the interval between these events, which is plotted in Fig. 1 D. The results confirm the impression from visual examination of the time-lapse videos, indicating that daughter cells polarize before start whereas mother cells polarize after start. Although effective for the Bem1 and Cdc24 probes, the CV quantification method was not successful for the Cdc42 probe (in unpolarized cells, Cdc42 is partly membrane associated, which raises the CV relative to the cytoplasmic Bem1 or Cdc24 probes). Nevertheless, visual examination suggested that as for the other polarity probes, Cdc42 polarization could be detected before start in many daughter cells, but always occurred after start in mother cells (Fig. 1, C and D). The prestart polarization observed in daughter cells may correspond to the previously reported “weak” polarization period observed in some wild-type diploid cells using the Bem1 probe (Wu et al., 2013), as well as the prestart polarization detected in wild-type haploid cells with a GTP-Cdc42 reporter (Lee et al., 2015).

A recent study reported that the axial bud-site selection protein Bud3 displayed Cdc42-directed GEF activity in vitro (Kang et al., 2014). Moreover, that study detected two waves of GTP-Cdc42 localization in haploid cells: an early wave immediately after cytokinesis that was dependent on Bud3, and a later (likely poststart) wave dependent on Cdc24. To assess whether the prestart polarization we detected was dependent on Bud3, we imaged cells lacking Bud3. *bud3Δ* homozygous diploids behaved similarly to wild-type diploids (Fig. 1, D and E). We also detected prestart polarization in haploid daughter cells, which was also not dependent on Bud3 (Fig. S3). Thus, the prestart polarization we detected was not dependent on Bud3. Possible explanations for the discrepancies between our and other studies are considered in the Discussion.

To assess whether prestart polarization might be influenced by the synchrony protocol, we also imaged unsynchronized cells. To avoid phototoxicity, these cells were imaged at somewhat lower spatiotemporal resolution. Nevertheless, it was readily apparent that as in the synchronized cells, the polarity marker Bem1 became polarized before start in daughter cells (Fig. 1, F and G). We conclude that polarization can precede full CDK activation.

Timing of polarization relative to cytokinesis

Mother and daughter cells differ in the duration of the prestart G1 interval: mothers have a short interval between cytokinesis and start, whereas daughter cells have a longer interval, reflecting the need to grow to a critical size to undergo start (Johnston et al., 1977; Di Talia et al., 2007). Thus, a possible explanation for the mother/daughter difference in the timing of polarization relative to start is that all cells polarize after some delay time following cytokinesis, and that the delay time is shorter than the time to start in daughter cells but longer than the time to start in mothers. This hypothesis would be consistent with prior studies

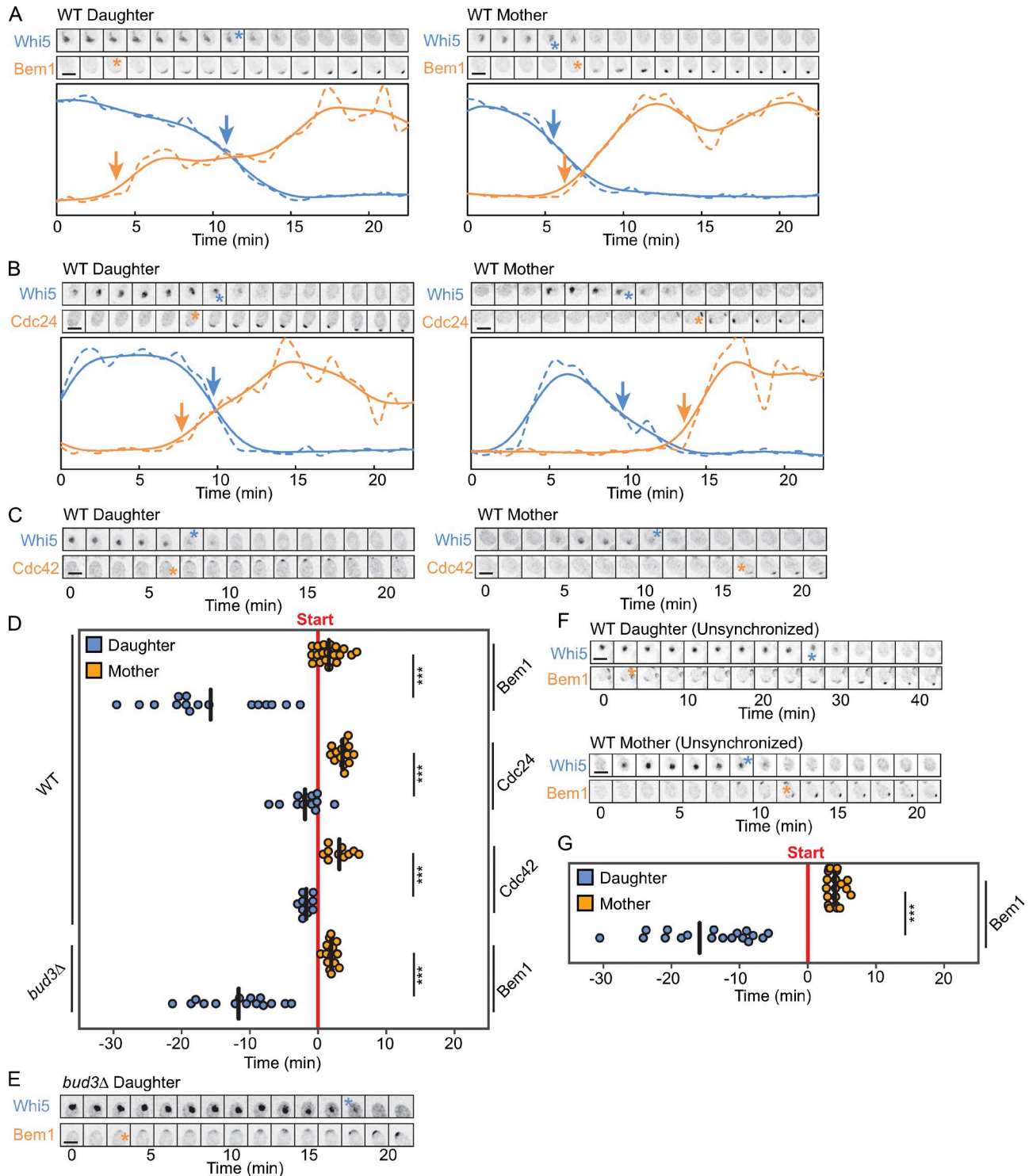


Figure 1. Timing of polarization relative to cell cycle start. Daughter cells polarize before start and mother cells polarize after start. **(A)** Maximum-projection montages of representative wild-type diploid mother and daughter cells expressing *Whi5*-GFP and *Bem1*-tdTomato (DLY19682), released from HU arrest and shown at 1.5-min intervals. Graph depicts pixel intensity CV (dashed lines, raw data; solid lines, smoothed spline fits). The *Whi5* CV (blue) reflects the concentration of *Whi5* in the nucleus, and the blue arrow indicates the time when the *Whi5* CV has dropped to 50% of its maximum (i.e., start). The *Bem1* CV (orange) reflects the concentration of *Bem1* at the polarity site, and the orange arrow indicates the initiation of polarization. Blue and orange asterisks mark the corresponding times of start and polarity onset on the montages. **(B)** Montages and graph as in A for cells of strain DLY21642 expressing *Whi5*-tdTomato and *Cdc24*-GFP. **(C)** Montages as in A for cells of strain DLY21457 expressing *Whi5*-GFP and *Cdc42*-mCherry^{SW}. **(D)** Timing of polarization relative to start for *Bem1*, *Cdc24*, and *Cdc42* probes. Each dot is one cell; line shows the average. Negative values indicate polarization takes place before start. For *Cdc42*, polarization timing was scored by eye. **(E)** Montages as in A for representative diploid *bud3Δ* daughter cell of strain DLY22159 expressing *Whi5*-tdTomato and *Bem1*-GFP. **(F)** Montages for cells from the same strain as in A but from asynchronous cultures. **(G)** Timing of polarization relative to start for unsynchronized cells (DLY19682). Scale bars, 5 μ m. ***, $P < 0.001$.

indicating that polarity-inhibitory pathways are triggered in G2/M and might need time to dissipate (Lew and Reed, 1993; Padmashree and Surana, 2001).

We used the arrival of Bem1 at the neck as a marker for the time of cytokinesis and measured the interval between cytokinesis and the onset of polarization in asynchronously proliferating cells. This interval was short in mother cells and longer in daughter cells (Fig. 2 A). Thus, there is not a fixed interval between cytokinesis and polarization. Nevertheless, these data are consistent with the idea that polarity can be triggered by one of two factors: either a delay that allows inhibitory factors from the previous G2/M to dissipate (triggering prestart polarization in daughters) or passage through start (triggering polarization in mothers). However, this hypothesis predicts that if the daughter cell prestart interval were shortened (e.g., by hydroxyurea arrest-release, which generates large daughter cells), then polarization should occur poststart in daughters as well as mothers. This was not the case. In synchronized daughter cells, the interval from cytokinesis to polarization was similar in mothers and daughters (Fig. 2 B), yet polarization nevertheless preceded start in daughters and followed start in mothers (Fig. 1).

Direct comparison of polarization timing in individual mother-daughter pairs after hydroxyurea arrest/release showed that whereas the mother cells generally passed start before the daughters, the daughter cells generally polarized before the mothers (Fig. 2 C). The most common pattern was that after cytokinesis, the daughter cell polarized first, then the mother cell went through start, then the mother cell polarized, and then the daughter went through start (Fig. 2 C). We conclude that although the short prestart G1 interval of mothers may be part of the reason why we see polarization poststart only in mother cells, there is also something about daughter versus mother cell identity, and not just the duration of the prestart interval, that affects the timing of polarization.

Polarization of Cdc42 effectors

The unexpected difference between polarization in mother cells and daughter cells prompted us to examine when Cdc42 effectors became polarized. Using Whi5 nuclear export as a marker for start, we monitored polarization of the PAKs Ste20 and Cla4, the formin Bni1 (Evangelista et al., 1997), the exocyst subunit Exo70 (Wu et al., 2010), and Gic1 (Brown et al., 1997; Chen et al., 1997). In daughter cells, we found that Ste20 was polarized before start, but all of the other effectors were polarized after start (Fig. 3, A–E). In mother cells, all probes polarized after start, as expected (Fig. 3 F). Thus, Ste20 appears to be unusual among Cdc42 effectors in its ability to polarize before start. For all of the other effectors, these findings raise the question: given the presence of a polarity site with concentrated Cdc42, Cdc24, Bem1, and Ste20 before start in daughter cells, why do the other effectors not accumulate there?

Cla4 and Ste20 are related PAKs that contain similar Cdc42-binding CRIB domains. Both CRIB domains suffice for interaction with GTP-Cdc42 in vitro (Gladfelter et al., 2001), so it is particularly surprising that Cla4 failed to polarize in prestart daughters. We confirmed that Cla4 polarized later than Bem1 (Fig. 4 A) and Ste20 (Fig. 4 B) in daughter cells, whereas Bem1 and Ste20 polarized at the same time (Fig. 4 C).

At later times (near the time of bud emergence), we noticed another unexpected difference between Ste20 and Cla4. Whereas Cla4 remained localized at the polarity site, Ste20 disappeared, reappearing later after bud emergence (Fig. 4 D). We considered the possibility that effectors might compete with each other for available GTP-Cdc42: if Ste20 has some advantage prestart and Cla4 has some advantage during bud emergence, such competition could explain our observations.

To test the competition hypothesis, we asked whether deletion of *STE20* would enable localization of Cla4 in prestart daughter cells, and whether deletion of *CLA4* would enable localization of Ste20 in cells undergoing bud emergence. We found that Cla4 did not localize to prestart daughters in the absence of Ste20 (Fig. 4, E and F), suggesting that Ste20 is not simply outcompeting the other effectors at that time. In contrast, Ste20 remained polarized (instead of disappearing) during bud emergence in cells lacking Cla4, consistent with the idea that Cla4 competes with Ste20 at this time (Fig. 4 G).

Because competition with Ste20 does not explain the inability of Cla4 to polarize before start, the simplest explanation for our observations would be that Cla4 requires G1 CDK activity to recognize Cdc42, whereas Ste20 does not. Consistent with that hypothesis, we observed polarization of Ste20 but not Cla4 in *cdc28-13* temperature-sensitive mutants after shift to the restrictive temperature (Fig. 4 H). Together, these findings suggest that Cla4 and other effectors, but not Ste20, require input from CDK to localize to the polarity site.

Prestart polarization requires positive feedback via Bem1 and Ste20

A recent study using optogenetics to locally activate Cdc42 suggested that prestart cells possessed a novel Bem1-independent positive feedback mechanism to concentrate active Cdc42 (Witte et al., 2017). In that study Bem1 was not detected at light-induced polarity sites before start, but we did observe Bem1 accumulation in daughter cells before start (Fig. 1 A). This prompted us to ask whether Bem1 was required for prestart polarization. We used the anchor-away method (Haruki et al., 2008) to promote inducible sequestration of Bem1 (Fig. 5 A). In this approach, addition of rapamycin generates tight binding of Bem1 to ribosomes, preventing Bem1 from accumulating at polarity sites (Woods et al., 2015, 2016). (Note that this strain bears a *TOR1* mutation that renders it resistant to the normal antiproliferative effects of rapamycin; Haruki et al., 2008.) Using Ste20-mCherry as a probe for polarization and Whi5-GFP to monitor cell cycle progression, we found that untreated cells of the anchor-away strain behaved like wild-type, with daughter cells polarizing Ste20 and Bem1 before Whi5 exit from the nucleus (Fig. 5, B and C). However, rapamycin treatment eliminated all detectable polarization of Ste20 or Bem1, either before or after start (Fig. 5 D; 0 of 42 cells polarized). Thus, Bem1 is polarized before start in daughter cells and is necessary for prestart polarization of Ste20.

Previous work indicated that Bem1 localization to the polarity site was dependent on the second SH3 domain of Bem1, which binds to the PAKs as well as other Cdc42 effectors (Irazoqui et al., 2003). As Ste20 is the only Cdc42 effector we detected at prestart polarity sites, we next asked whether prestart polarization

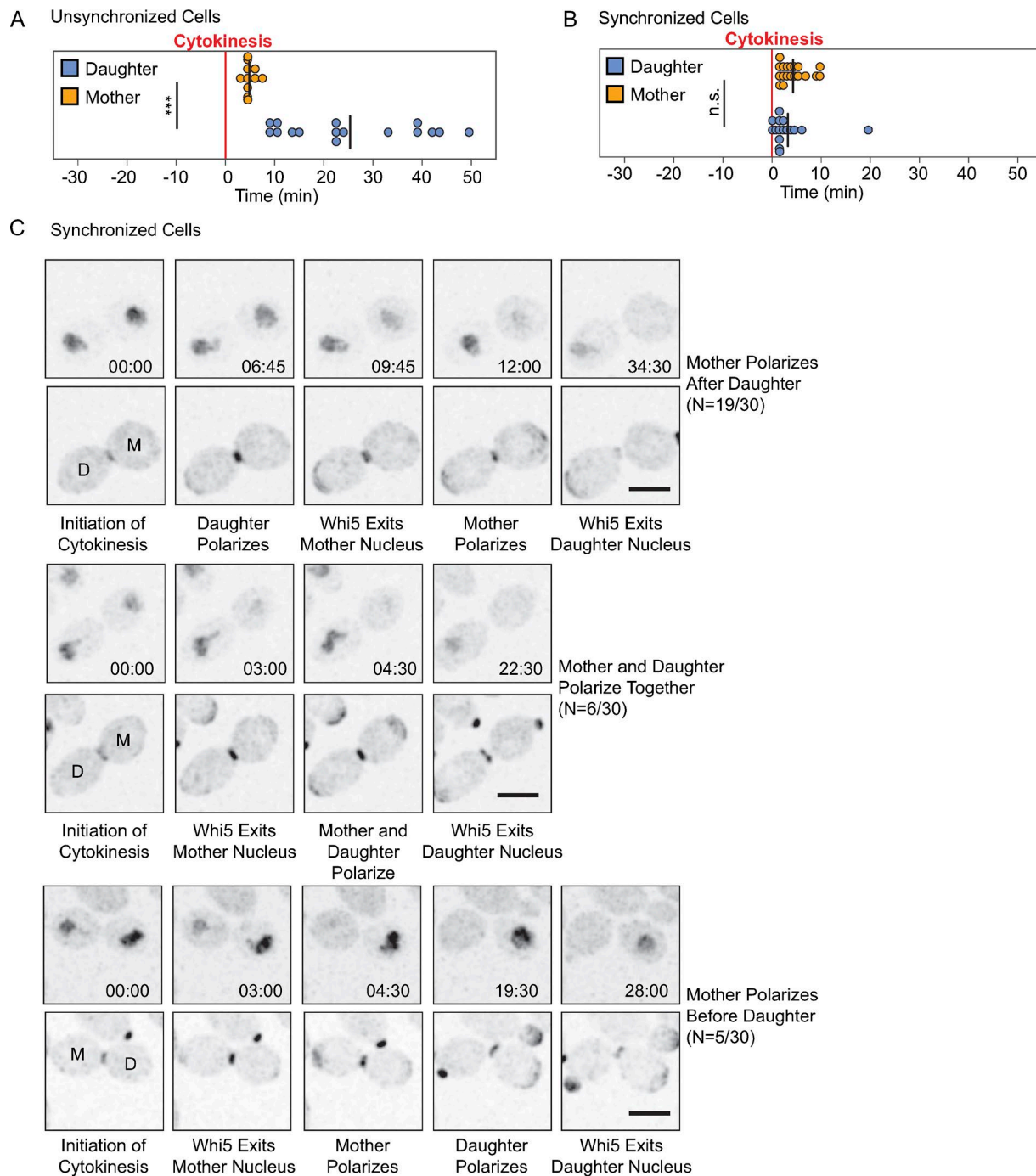


Figure 2. Timing of polarization relative to cytokinesis. Videos of diploid cells expressing Whi5-GFP and Bem1-tdTomato (DLY19682) were reanalyzed to score the time interval between cytokinesis (the first time point when Bem1 was concentrated at the neck) and polarization (scored as in Fig. 1). **(A)** In asynchronous cells, mothers polarized before daughters. **(B)** In cells synchronized by HU arrest-release, mothers and daughters polarized at similar times after cytokinesis. **(C)** Representative examples of mother-daughter pairs from the HU arrest-release experiment. Three patterns were detected. Top: In most cases, daughter cells polarized before mothers even though mothers passed start before daughters. Middle: Mother and daughter polarized simultaneously, after the mother passed start but before the daughter passed start. Bottom: The mother passed start and polarized before the daughter polarized. Scale bars, 5 μ m. n.s., $P > 0.01$; ***, $P < 0.001$.

was dependent on Ste20. Mutants lacking Ste20 failed to polarize Bem1 (Fig. 5 E), Cdc24 (Fig. 5 F), or Cdc42 (Fig. 5 G), before start. Instead, polarization of all markers occurred after start in both mother and daughter *ste20* mutant cells (Fig. 5 H). Thus, Ste20 is also required for prestart polarization.

Ste20 is thought to participate in positive feedback by mediating interactions between GTP-Cdc42 and Bem1 (Kozubowski et al., 2008). Ste20 has also been implicated in Bud8-dependent distal budding of diploid cells (Sheu et al., 2000). Prestart polarization almost always occurred as a broad crescent at the distal

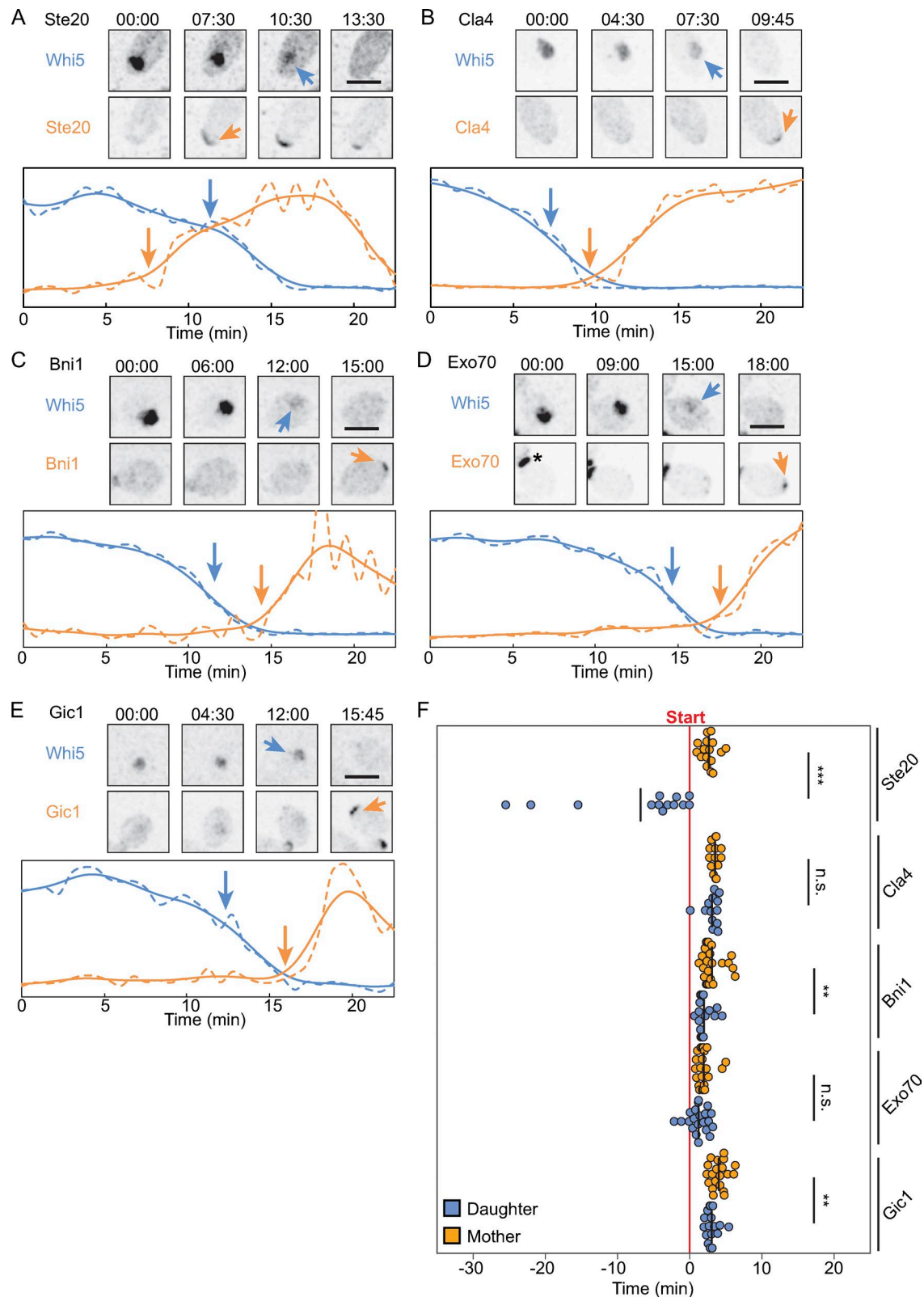


Figure 3. Timing of Cdc42 effector polarization. In daughter cells, Ste20 polarizes before start but Cla4, Bni1, Exo70, and Gic1 polarize after start. **(A–E)** Cells of strains DLY19685 (A; Ste20-mCherry), DLY20043 (B; Cla4-GFP), DLY22205 (C; Bni1-GFP), DLY22190 (D; Exo70-GFP), and DLY22856 (E; Gic1-mNeonGreen) were analyzed as in Fig. 1. Maximum-projection images from selected time points are shown, with polarization indicated by orange arrows and start (50% decrease in Whi5 CV) by blue arrows. In D, the cytokinesis site is marked with a black asterisk to avoid confusion with the polarity site. **(F)** Timing of polarization relative to start for the strains shown in A–E. Scale bars, 5 μ m. n.s., $P > 0.01$; **, $P < 0.01$; ***, $P < 0.001$.

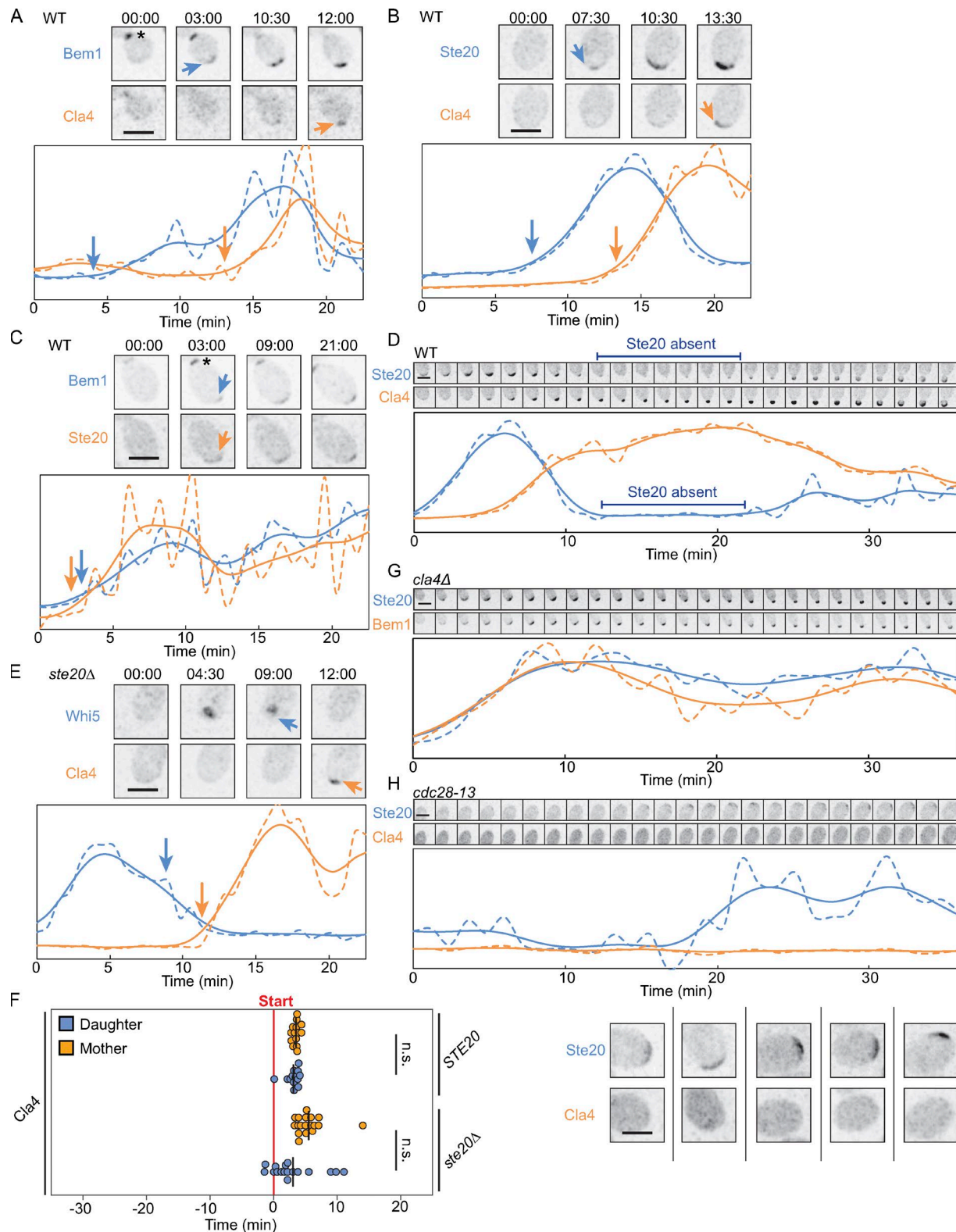


Figure 4. Comparison of Ste20 and Cla4 polarization. (A) Bem1 polarizes before Cla4. Representative daughter cell from strain DLY20200 expressing Bem1-tdTomato and Cla4-GFP, displayed as in Fig. 2. Maximum-projection images from selected time points are shown, with polarization indicated by orange (Cla4) or blue (Bem1) arrows. The cytokinesis site is marked with a black asterisk. This ordering was observed for 16/16 daughter cells. (B) Ste20 polarizes before Cla4. Representative daughter cell from strain DLY19547 expressing Ste20-mCherry and Cla4-GFP. Polarization is indicated by orange (Cla4) or blue (Ste20) arrows. This ordering was observed for 17/17 daughter cells. (C) Bem1 and Ste20 polarize at similar times. Representative daughter cell from strain DLY19804 expressing Bem1-GFP and Ste20-mCherry. The cytokinesis site is marked with a black asterisk. This was observed for 16/18 daughter cells. (D) Ste20 is absent from the polarity site during bud emergence (indicated by blue bar). Longer timeframe montage (1.5-min intervals) and graph for the same cell as in B. This behavior was observed for 11/11 cells. (E) Cla4 still polarizes after start in *ste20Δ* daughter cells. Representative daughter cell from *ste20Δ*

tips of daughter cells, which are marked with a similar crescent of Bud8 (Harkins et al., 2001). Bud8 promotes distal polarization via Rsr1, which interacts with Cdc24. We found that in *rsr1Δ* mutants, polarization was detected only after start in both mother and daughter cells (Fig. 6, A and F). Similarly, polarization was detected after start in *cdc24-4* mutants (incubated at permissive temperature), harboring a Cdc24 GEF that cannot interact with Rsr1 (Fig. 6, B and F; Shimada et al., 2004). Thus, prestart polarization to the distal pole in daughters requires Rsr1–Cdc24 interaction.

To distinguish whether the requirement for Ste20 in prestart polarization reflects Ste20-mediated Bud8 regulation or Ste20-mediated positive feedback, we generated separation-of-function mutants. If Ste20 provides positive feedback by linking GTP-Cdc42 to Bem1, then mutants that impair either Ste20–GTP-Cdc42 interaction or Ste20–Bem1 interaction should be defective in prestart polarization. Binding of Ste20 to GTP-Cdc42 is mediated by the Cdc42/Rac interactive binding (CRIB) domain of Ste20 (Leberer et al., 1997). The CRIB domain also has an auto-inhibitory function that suppresses Ste20 kinase activity (Moskow et al., 2000; Lamson et al., 2002). Thus, a variant of Ste20 lacking the CRIB domain is unable to bind Cdc42 but has constitutive kinase activity. Binding of Ste20 to the second Bem1 SH3 domain is mediated by adjacent proline-rich motifs (PSRPAPKPP) in Ste20 and is impaired when the two central prolines are mutated (Winters and Pryciak, 2005). We found that both Ste20^{ΔCRIB} and Ste20^{PP-GA} rescued the distal budding defect in diploids (Fig. 6 C), so these mutants block positive feedback without impairing Bud8 regulation. Unlike in cells with wild-type Ste20, daughter cells polarized after start in diploids with Ste20^{ΔCRIB} or Ste20^{PP-GA} as the sole source of Ste20 (Fig. 6, D and E). Thus, prestart polarization requires positive feedback via Bem1 and Ste20, as well as Rsr1–Cdc24 interaction.

Why does prestart polarization require Rsr1 when poststart polarization does not?

Seeing as Rsr1 is dispensable for polarization after start, why is it required for polarization in prestart cells? Rsr1 is thought to act by concentrating a small amount of Cdc24 at sites designated by landmark proteins such as Bud8 (Park and Bi, 2007; Wu et al., 2013). In experiments involving acute withdrawal of Bem1 to inactivate positive feedback, there is no detectable polarization despite the presence of intact Rsr1 and Cdc24 (Fig. 4; Jost and Weiner, 2015; Woods et al., 2015), suggesting that the Cdc24 recruited by Rsr1 is a small fraction of that recruited by positive feedback. Under what circumstances might this small amount of localized Cdc24 become essential for polarity? And why would that change after CDK activation?

We imagined two broad scenarios to explain how CDK activation might alter polarity requirements. One possibility is that the strength of positive feedback is increased upon CDK activation. A specific version of this scenario is the proposal that association of Bem1 with Cdc24 is stimulated by CDK activity (Witte et al., 2017). Alternatively, positive feedback may be constitutively “on” without need for CDK activity, but prevented from being effective by a polarity “antagonist” before CDK activation. Then, the antagonist would be inactivated by the CDK to allow subsequent polarization. A specific version of that scenario is supported by the finding that the Cdc42-directed GAPs, Rga2 and Bem3, are phosphorylated and perhaps inactivated by G1 CDK activity (Knaus et al., 2007; Sopko et al., 2007).

To investigate whether these hypotheses could plausibly explain our findings, we turned to computational modeling. For positive feedback, we used a model originally developed by Goryachev and Pokhilko (2008), adjusted as described (Wu et al., 2015). To model Rsr1 action, we assumed that the landmarks and Rsr1 would promote recruitment of a small amount of GEF (just 1% of that seen in the center of a polarity site) to a defined region of the cortex (Wu et al., 2013).

To adjust the strength of positive feedback, we altered the association rate for binding of Bem1 to Cdc42–GTP (Fig. 7 A). As expected, there was a threshold below which the binding was insufficient to promote polarization by positive feedback alone (Fig. 7 B). Strikingly, however, addition of the very weak Rsr1 pathway rescued robust polarization below this threshold, revealing a parameter regimen in which polarity required both Rsr1 and positive feedback (Fig. 7 B). Similarly, increasing GAP activity above a threshold was sufficient to block polarization by positive feedback alone (Fig. 7 C). However, addition of Rsr1-localized GEF rescued robust polarization above this threshold, again revealing a parameter regimen in which polarity required both Rsr1 and positive feedback (Fig. 7 C). Exploring different combinations of these parameters illustrated a broad regimen in which a small amount of local GEF activation by Rsr1 could sustain a positive feedback-driven polarity peak in conditions that would fail to polarize without Rsr1 (Fig. 7 D).

Similar results were obtained using more complex models that incorporated negative feedback as well as positive feedback (Kuo et al., 2014; Fig. 7 E–G). Thus, in principle, our observations might be explained by assuming that Ste20 provides only weak positive feedback before start, or that GAP activity is higher before start, or both.

Bypassing regulation of the assembly of Bem1 complexes

One way for CDK activity to strengthen positive feedback would be to stimulate assembly of the PAK–Bem1–Cdc24 complex (Witte et al., 2017). If that were responsible for the CDK requirement

strain DLY21719 expressing Whi5–tdTomato and Cla4–GFP. (F) Timing of Cla4 polarization relative to start in wild-type (DLY20043) and *ste20Δ* (DLY21719) cells. (G) Ste20 remains polarized during bud emergence in *cla4Δ* cells. Longer timeframe montage (1.5-min intervals) and graph from a representative *cla4Δ* daughter cell of strain DLY20196 expressing Ste20–GFP and Bem1–tdTomato. This behavior was observed for 21/21 cells. (H) Ste20 but not Cla4 becomes polarized in *cdc28-13* cells at restrictive temperature. Top: Longer timeframe montage (1.5-min intervals) and graph from a representative *cdc28-13* cell of strain DLY22332 expressing Ste20–mCherry and Cla4–GFP. Bottom: Other example snapshots of single cells from the same experiment, showing Ste20 and Cla4 signals for the same cells. This behavior was observed for 37/40 cells. Scale bars, 5 μm. n.s., $P > 0.01$.

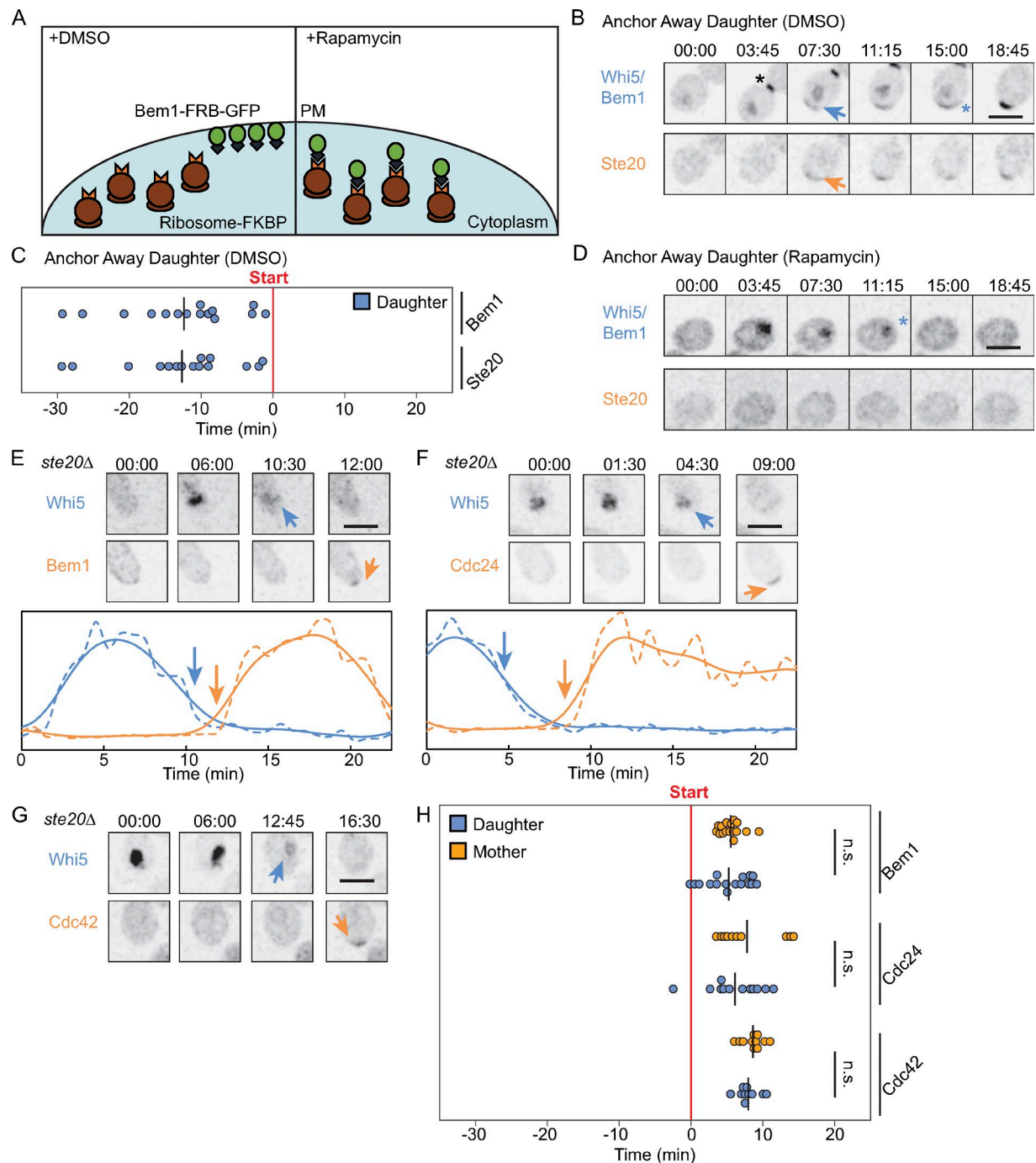


Figure 5. Bem1 and Ste20 are required for prestart polarization. (A) Anchor-away technique. Without rapamycin (left), Bem1 localizes to the polarity site. With rapamycin (right), Bem1 is sequestered to the ribosomes. (B) Control: Anchor-away strain in the absence of rapamycin. Montage of representative cell of strain DLY22958 expressing Ste20-mCherry, Whi5-GFP, and Bem1-FRB-GFP. Arrows indicate polarization of Bem1 (blue) and Ste20 (orange). Blue asterisk indicates Whi5 nuclear exit (start). Black asterisk indicates the cytokinesis site. (C) Timing of Ste20 and Bem1 polarization relative to start in the same strain. Bem1 and Ste20 polarize before start in daughter cells. (D) Montage of representative cell of the same strain in the presence of rapamycin: neither Bem1 nor Ste20 become polarized. Asterisk indicates Whi5 nuclear exit (start). (E–G) Polarization of Bem1 (E, DLY21710), Cdc24 (F, DLY21666), and Cdc42 (G, DLY21597) in *ste20Δ* daughter cells. In all cases, polarization (orange arrow) now occurs after start (blue arrow). Display as in Fig. 2. (H) Timing of polarization relative to start for Bem1, Cdc24, and Cdc42 in *ste20Δ* cells (strains as in E–G). Scale bars, 5 μ m. n.s., $P > 0.01$.

for polarization, then fusing components of the complex to each other would be expected to bypass the need for CDK in Cdc42 regulation during the cell cycle.

Accumulation of GTP-Cdc42 leads to PAK activation, which in turn leads to phosphorylation of Cdc24 (Gulli et al., 2000;

Bose et al., 2001; Wai et al., 2009). We used the accompanying mobility shift of Cdc24 to follow Cdc42 activation through the cell cycle in synchronized cells. Cells were arrested in G1 with mating pheromone, released into the cell cycle, and rearrested in G2/M by addition of nocodazole. In wild-type

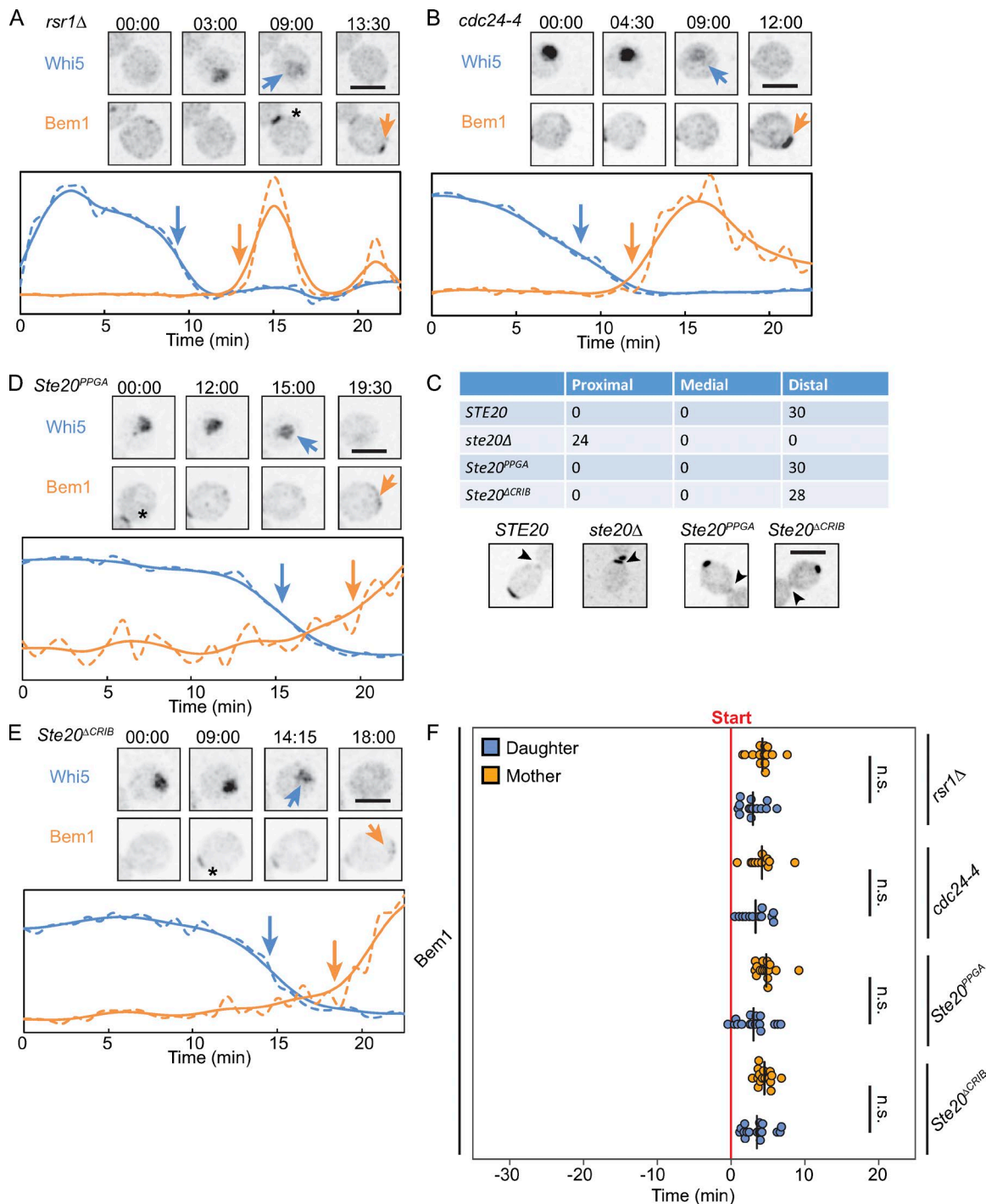


Figure 6. Rsr1- and Ste20-mediated positive feedback are required for prestart polarization. (A) Bem1 polarizes after start in *rsr1Δ* daughter cells. Selected time points (display as in Fig. 2) of representative daughter cell of *rsr1Δ* strain DLY19237 expressing Bem1-tdTomato and Whi5-GFP. **(B)** Similar behavior in *cdc24-4* (DLY21693) daughter cells. **(C)** *ste20Δ* cells exhibit a distal budding defect that is rescued by the *Ste20^{PPGA}* and *Ste20^{ΔCRIB}* alleles. Arrowheads indicate site of cytokinesis (proximal pole in next cell cycle). Strains DLY19682, DLY21710, DLY21799, and DLY21980. **(D)** Bem1 polarizes after start in *Ste20^{PPGA}* daughter cells (DLY21979). **(E)** Bem1 polarizes after start in *Ste20^{ΔCRIB}* daughter cells (DLY21980). **(F)** Timing of Bem1 polarization relative to start for strains from A–E. The cytokinesis site is marked with a black asterisk where applicable. Scale bars, 5 μ m. n.s., $P > 0.01$.

cells, Cdc24 became phosphorylated in late G1/S and then dephosphorylated in G2/M (Fig. 8 A). Fusion of Cdc24 to the PAK-binding region of Bem1 (expected to compensate for loss of Bem1–Cdc24 interaction) did not affect the phosphoregulation of Cdc24 through the cell cycle (Fig. 8 B). Similarly,

fusion of the PAK Cla4 to Bem1 (expected to compensate for the loss of Cla4–Bem1 interaction) or to Cdc24 (expected to compensate for the loss of both Cla4–Bem1 and Bem1–Cdc24 interactions) failed to alter the G1-phase regulation of Cdc24 phosphorylation: Cdc24 was dephosphorylated at 15 min and

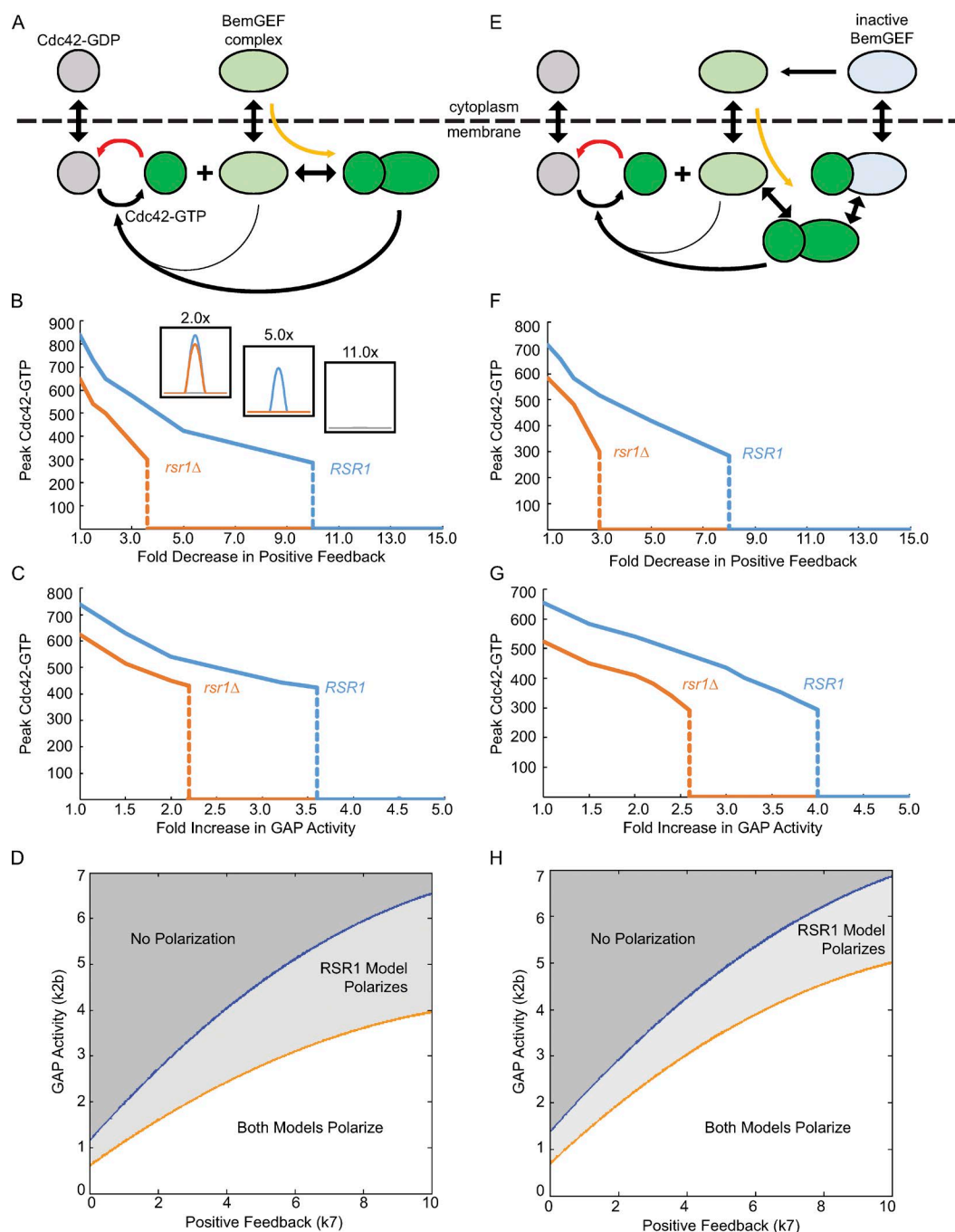


Figure 7. Computational modeling reveals parameter regimen in which Rsr1-localized GEF is required for effective polarization. (A) Cartoon of the reactions in the model with positive feedback. GDP-Cdc42 (gray) can transit between the cytoplasm (where diffusion is rapid) and the membrane (where diffusion is slow), assisted by GDI. PAK-Bem1-GEF complexes (light green) also transit between membrane and cytoplasm, and can bind GTP-Cdc42 (dark green) at the membrane. GTP-Cdc42 hydrolyzes bound GTP to yield GDP-Cdc42, assisted by GAPs. At the membrane, Bem1-GEF complexes promote conversion of GDP-Cdc42 to GTP-Cdc42, which can then bind further Bem1-GEF complexes, providing positive feedback. **(B)** Decreasing positive feedback (by decreasing rate of the yellow reaction arrow in A) decreases the peak steady-state GTP-Cdc42 concentration (solid lines) until the peak collapses (dashed lines). Orange line depicts simulation results for model in A. Blue line depicts results for simulations in which there is an additional localized GTP-Rsr1 that recruits additional GEF (~1% of peak level) to the local membrane. Inset: Shape of GTP-Cdc42 peaks for the model with (blue) and without (orange) Rsr1 at twofold, fivefold, and 11-fold decreases in positive feedback. **(C)** Increasing GAP activity (red arrow in A) decreases the peak steady-state GTP-Cdc42 concentration (solid lines) until the peak collapses (dashed lines). Orange (without Rsr1) and blue (with Rsr1) simulations as in B. **(D)** Phase diagram indicating parameter space in which polarity fails (dark gray), requires only positive feedback (white), or requires both Rsr1 and positive feedback (light gray). **(E)** Cartoon of the reactions in the model with positive and negative feedback. This model is identical to that in A but has an additional reaction in which the GEF becomes phosphorylated (blue) by PAK. Phosphorylated GEF is assumed to be inactive until it is released into the cytoplasm and dephosphorylated. This provides negative feedback because GTP-Cdc42 (via PAK) promotes inactivation of its GEF. **(F)** Analysis as in B for the model with negative feedback. **(G)** Analysis as in C for the model with negative feedback. **(H)** Phase diagram as in D for the model with negative feedback.

then phosphorylated, as in wild type (Fig. 8, C and D). Thus, it appears that control of Cdc42 GTP-loading in G1 can occur even when fusion proteins enforce constitutive assembly of the PAK-Bem1-Cdc24 complex.

Unexpectedly, fusion of the PAK Cla4 to Bem1 (Fig. 8 C) or to Cdc24 (Fig. 8 D) resulted in elevated Cdc24 phosphorylation during the G2/M arrest. These findings suggest that normal dephosphorylation of Cdc24 in G2/M requires disassembly of the complex (and specifically the Cla4-Bem1 link).

Role of Cdc42-directed GAPs

To test the idea that high GAP activity may be responsible for restraining polarization before CDK-mediated GAP inactivation, we examined the timing of polarization in cells lacking the GAPs Rga2 and Bem3 (these cells still contain the GAPs Bem2 and Rga1). Hydroxyurea treatment of mutant cells led to aberrant cell morphologies (not depicted), so in this case we imaged asynchronous cells. We found that loss of these GAPs advanced the timing of Ste20 polarization, in both daughters and mothers (Fig. 8, E and F). Some mother cells were now seen to polarize prestart, although daughter cells still polarized earlier than mother cells. We conclude that GAP activity provided by Rga2 and Bem3 contributes to the suppression of polarization before start.

Discussion

Polarization of Cdc42 before start

Most, although not all (Padmashree and Surana, 2001; Lee et al., 2015), previous studies concluded that Cdc42 polarization was dependent on G1 CDK activity (Gulli et al., 2000; Jaquenoud and Peter, 2000; Butty et al., 2002; Wedlich-Soldner et al., 2004). Here we show that the timing of polarization differs in mother and daughter cells: daughter cells polarize before start, whereas mother cells polarize after start. Although different probes might be detected at different times owing to differences in probe abundance and thresholds for detection, these conclusions hold for Cdc42, Cdc24, Bem1, and Ste20 probes, in both diploid and haploid cells, and in synchronized as well as asynchronous cell populations.

Our findings are fully consistent with those of a recent study using a CRIB-domain GTP-Cdc42 reporter to image polarization in haploid cells (Lee et al., 2015). In haploids, the prestart polarization was seen to “drift” around a ring at the previous cytokinesis site (Lee et al., 2015), whereas in diploids, we observed prestart polarization in a crescent at the distal tip of the daughters (opposite the cytokinesis site). These locations are populated by transmembrane landmark proteins in haploid (Axl2 in a ring at the neck) and diploid (Bud8 in a crescent at the distal tip) cells that recruit Bud5, the GEF for Rsr1, to those locations (Bi and Park, 2012). We found that Rsr1 was required for prestart polarization, although we cannot rule out the possibility that a weaker prestart polarization occurs at mobile locations, as detected in *rsr1* haploids (Lee et al., 2015). GTP-Rsr1 binds to both Cdc24 (Zheng et al., 1995) and Cdc42 (Kozminski et al., 2003), and we found that a *cdc24* mutant unable to bind Rsr1 also failed to exhibit prestart polarization. We conclude that wild-type daughter cells polarize Cdc42 to landmark-designated sites before start, and that

this prestart polarization involves Rsr1-mediated recruitment of Cdc24 to those sites.

Another study reported an early wave of polarization at the time of cytokinesis, detected with the GTP-Cdc42 reporter (Kang et al., 2014). This early polarization was dependent on the GEF Bud3, and not on Cdc24. Cdc42, Cdc24, and Bem1 (as well as several Cdc42 GAPs; Caviston et al., 2003) were known to concentrate at the cytokinesis site at that time, although previous work had not detected GTP-Cdc42 there (Atkins et al., 2013). Indeed, activation of Cdc42 at the neck during cytokinesis would be odd given considerable evidence suggesting that active Cdc42 at the neck can interfere with cytokinesis (Atkins et al., 2013; Onishi et al., 2013). We did not detect Ste20 at the cytokinesis site, even though Ste20 can polarize prestart and contains a CRIB domain, as does the GTP-Cdc42 reporter. It is possible that some other factor prevents Ste20 from recognizing GTP-Cdc42 at that time. Alternatively, it may be that the reporter artificially enhances the level of Cdc42 at the cytokinesis site by trapping GTP-Cdc42 that would otherwise be eliminated by GAPs. In either case, the prestart polarization documented in this work was dependent on Cdc24 and independent of Bud3.

A remaining open question concerns the basis for the difference in polarization timing between mother and daughter cells. One possibility we considered is that a polarity-inhibitory pathway left over from the previous mitosis (Lew and Reed, 1993; Padmashree and Surana, 2001) needs some time to dissipate before polarity can occur. Because mother cells proceed through start rapidly, there would be insufficient time in prestart G1 for mother cells to polarize. However, we found that the mother-daughter difference (poststart vs. prestart polarization) persisted after arrest/release synchronization, even though the large synchronized mothers and daughters have similar (short) intervals between cytokinesis and polarization. We conclude that daughter cells, which are known to enact a distinct transcriptional program from mothers (Bobola et al., 1996; Jansen et al., 1996; Sil and Herskowitz, 1996; Colman-Lerner et al., 2001; Nelson et al., 2003; Di Talia et al., 2009), have an enhanced intrinsic capacity to polarize.

Regulation of Cdc42 polarization by G1 CDK activity

Although daughter cells can polarize before start, our findings clearly indicate that the requirements for polarization are different before and after start. Before start, polarization was dependent on Rsr1 and Ste20, whereas after start it was not. Thus, G1 CDK activity makes it easier for cells to polarize.

How might G1 CDKs regulate polarization? Biochemical experiments indicated that Cdc28 can phosphorylate PAKs, Bem1, and Cdc24 (Oda et al., 1999; Han et al., 2005; McCusker et al., 2007), and recent findings based on colocalization suggested that Bem1-Cdc24 interaction may require G1 CDK activation (Witte et al., 2017). However, we found that Bem1 and Cdc24 both localized to the polarity site before start in daughters, and that prestart polarization required Ste20 and Bem1 in a manner consistent with the known positive feedback pathway (Kozubowski et al., 2008; Johnson et al., 2011). These findings are most easily explained by positing that Bem1 and Cdc24 do interact before start. Moreover, we found that fusing Bem1 to Cdc24, or fusing the PAK Cla4 to

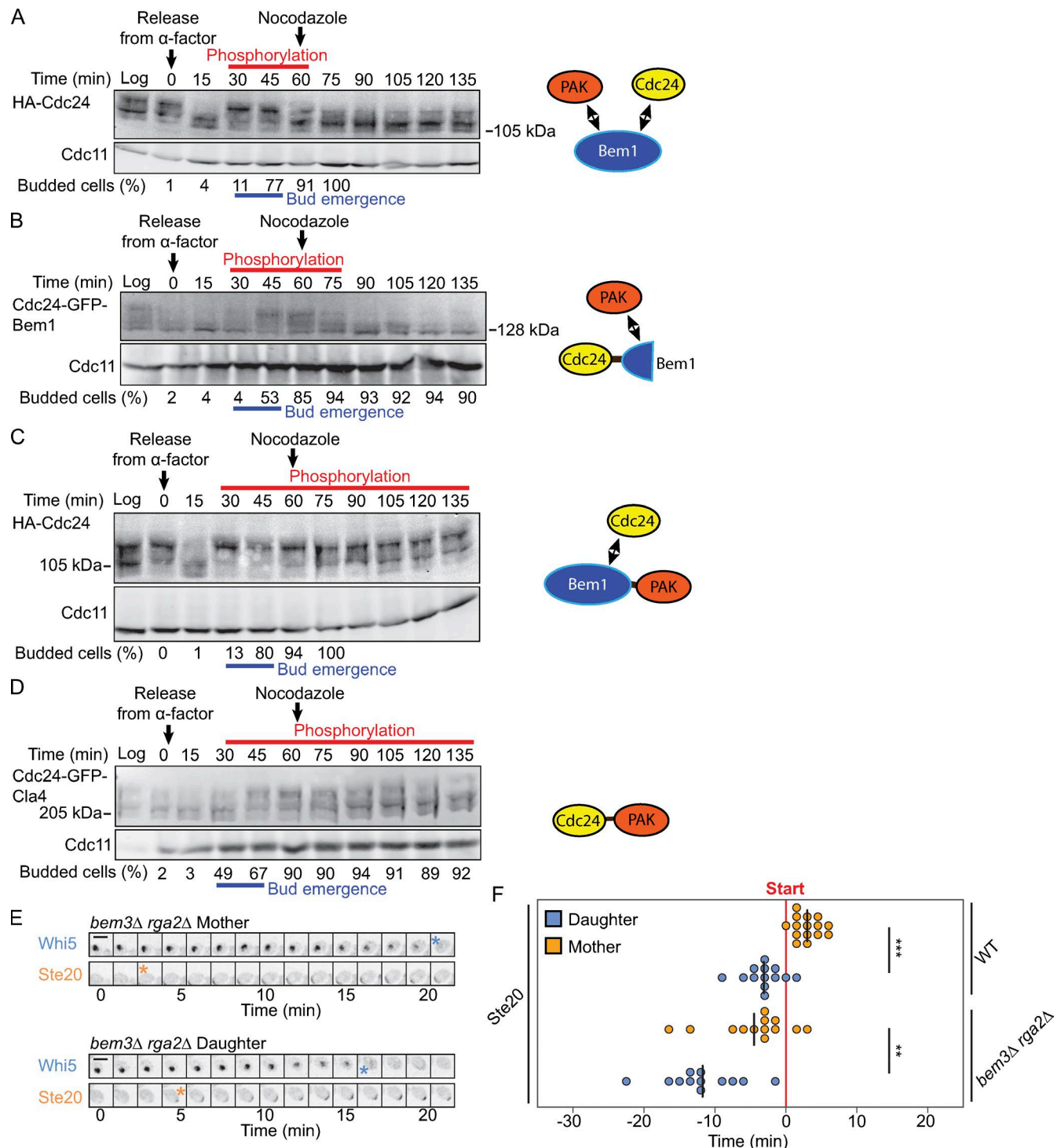


Figure 8. Roles of PAK-Bem1-GEF interactions and GAPs Rga2 and Bem3. (A–D) Cdc24 phosphorylation is mediated by PAKs and provides a readout of GTP-Cdc42 levels through the cell cycle. Phosphorylation of Cdc24 was assessed by mobility shift in SDS-PAGE as detected by Western blot of lysates from cells synchronized by α -factor G1 arrest-release into nocodazole arrest in G2/M. Percentage of cells budded is shown below the loading control (Cdc11). Red lines indicate Cdc24 phosphorylation. Blue lines indicate bud emergence. Cartoons (right) indicate binding (arrows) or fusions (black lines) between components. (A) Control: HA-Cdc24 phosphorylation in wild-type cells (DLY11474) rises at the time of bud emergence and decreases in G2/M. (B) Similar dynamics are observed in cells (DLY11522) expressing a Cdc24-Bem1 fusion protein. (C) Enforcing Bem1-Cla4 interaction prevents Cdc24 dephosphorylation in cells (DLY11410) expressing a Bem1-Cla4 fusion. (D) Enforcing Bem1-Cla4 interaction prevents Cdc24 dephosphorylation in cells (DLY11566) expressing a Cdc24-Cla4 fusion. (E) Ste20 polarizes before start in both mother and daughter cells lacking GAPs Bem3 and Rga2. Montage (1.5-min intervals) of representative cells of *bem3 Δ rga2 Δ* strain DLY21702. (F) Timing of Ste20 polarization relative to start in unsynchronized wild-type (DLY19685) and *bem3 Δ rga2 Δ* (DLY21702) cells. Scale bars, 5 μ m. **, $P < 0.01$; ***, $P < 0.001$.

Cdc24, did not bypass regulation of Cdc24 phosphorylation in G1, indicating that other pathways for regulation of polarity must act even in cells where dissociation of the PAK-Bem1-Cdc24 complex is not an option.

An attractive candidate pathway for CDK-mediated regulation of polarity operates via Cdc42-directed GAPs. The GAPs Rga2 (Sopko et al., 2007) and Bem3 (Knaus et al., 2007) are phosphorylated by G1 CDKs, and nonphosphorylatable mutants exhibit enhanced toxicity upon overexpression. This indirect evidence suggested that Rga2 and Bem3 phosphorylation could inhibit their activity, leading to the hypothesis that high GAP activity before start would block polarization, and CDK-mediated GAP inhibition would allow polarization. Computational modeling supported the idea that with intermediate GAP activity sufficient to prevent spontaneous polarization via positive feedback alone, a weak Rsr1-mediated localization of Cdc24 to landmark-designated sites could promote robust polarization. Moreover, we found that deletion of two GAPs, *RGA2* and *BEM3*, advanced the timing of polarization in both mothers and daughters. These findings are consistent with the hypothesis that G1 CDK activity regulates polarization by inhibiting Cdc42-directed GAPs (Fig. 9).

Regulation of Cdc42 effector localization

Even though daughter cells could polarize before start, budding never took place until well after start (Lai et al., 2018). This observation suggested a qualitative difference in the ability of prestart and poststart polarity sites to trigger downstream events. Among a panel of Cdc42 effectors, we found that Cla4, Bni1, Exo70, and Gic1 polarized after start even in daughter cells. In contrast, Ste20 polarized before start. In fact, Ste20 was required to mediate positive feedback to enable prestart polarization.

The (so far) unique behavior of Ste20 may reflect the fact that unlike the other Cdc42 effectors, Ste20 is required for signal transduction during mating (haploids) and pseudohyphal growth (diploids; Leberer et al., 1992; Mösch et al., 1996). For haploids, pheromone-initiated signals must be transmitted before start to promote the G1 arrest needed for mating, and a similar need for interpretation of nutrient signals in prestart G1 may apply for diploids. Thus, it may be important to maintain a signaling-competent pool of Cdc42-activated Ste20 in prestart cells. Because Ste20 can participate in positive feedback, that may lead to prestart polarization.

For the remaining effectors, the delay between prestart polarization of Cdc42/Cdc24/Bem1/Ste20 and poststart polarization of the other effectors suggested that G1 CDK activity triggers a change that allows the effectors to localize to the Cdc42-enriched sites (Fig. 9). Consistent with that hypothesis, we observed polarization of Ste20 but not Cla4 in *cdc28* temperature-sensitive mutants. CDKs may phosphorylate the effectors or other interacting proteins to enable binding to GTP-Cdc42. Alternatively, effectors may be able to bind GTP-Cdc42 at any time, but need additional regulation to enable membrane binding, which is important for Cdc42 effector localization (Takahashi and Pryciak, 2007). Although further work will be required to dissect the mechanism, this work identifies CDK-mediated regulation of effector localization as a major novel locus for cell cycle control of cell polarity.

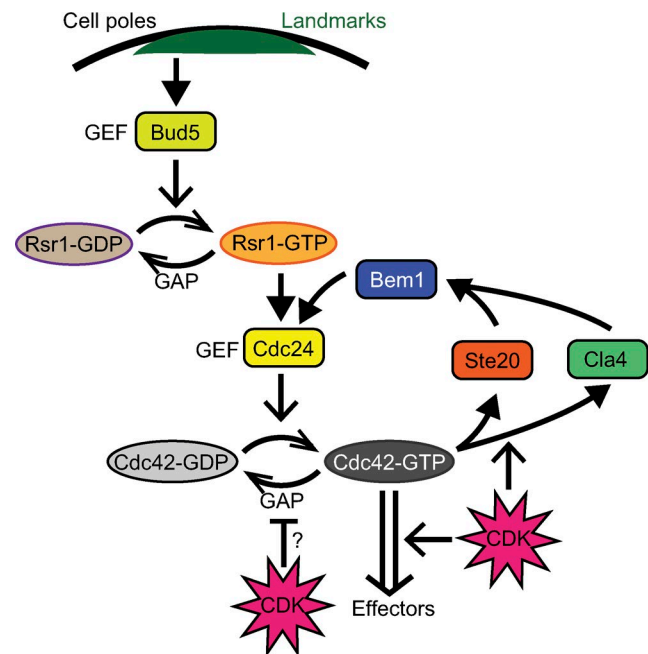


Figure 9. **Polarity establishment proteins and pathways as discussed in the Introduction.** Our findings support two loci for G1-CDK-mediated control of polarization: inhibition of Cdc42-directed GAPs and enabling of the localization of many effectors (with Ste20 as a conspicuous exception) to sites enriched for Cdc42.

Materials and methods

Yeast strains

Standard molecular and yeast genetic methods were used for strain construction. All yeast genetic modifications via homologous recombination were confirmed by appropriate PCR and sequencing using the genomic DNA of transformed yeast strains as templates. Yeast strains are listed in Table S1.

The following alleles have been described previously: Cla4-GFP (Wild et al., 2004), Bem1-GFP (Kozubowski et al., 2008), Bem1-tdTomato and Cdc24-GFP (Howell et al., 2012), Cdc24^{APB1}-GFP-Bem1(SH3, CI), Cdc24^{APB1}-GFP-Cla4, and Bem1-GFP-Cla4 (Kozubowski et al., 2008), Whi5-GFP and Htb2-mCherry (Doncic et al., 2011), *rsr1::TRP1* (Howell et al., 2009), *cdc24-4* (Sloat et al., 1981), *cla4::NAT* and *ste20::HPH* (Weiss et al., 2000), Cdc42-mCherry^{SW} (Woods et al., 2015), 3HA-GFP-Bni1 (Chen et al., 2012), *bud3::HIS3* (Gao et al., 2007), and *bem3::TRP1* and *rga2::KanMX* (Caviston et al., 2003).

Whi5-tdTomato was introduced by transforming cells with plasmid pDLB4249 (pNI8-WHI5(last 300 bp)-tdTomato-TEF1t-CaURA3-TEF1t-WHI5 3'UTR, a gift from C. Tang [Peking University, Beijing, China]) digested with HindIII. Ste20-mCherry and Ste20-GFP were generated by the PCR-based gene modification method (Longtine et al., 1998). Briefly, primers with 50 bp of *STE20* C-terminus and 3' UTR homology were used to amplify the pFA6 mCherry or GFP transformation module from pDLB2866 and pDLB52, respectively. The PCR product was then purified and transformed into strains with wild-type *STE20* via standard transformation methods. Proper integration was confirmed by sequencing and fluorescence microscopy. Exo70-GFP

was generated in a similar fashion using an amplification of the pFA6 GFP transformation module from pDLB3524.

Ste20^{PP-GA} and Ste20^{ΔCRIB} were generated by digesting pDLB4347 (pRS306-STE20) with BamHI and KsI to excise a portion of *STE20*. Corresponding fragments containing the PP-GA and ΔCRIB mutations were generated using the same restriction enzymes from pDLB2791 and pDLB3147, respectively, which contain Ste20 mutants as reported (Winters and Pryciak, 2005). These mutant fragments were then ligated into the cut pDLB4347. Gic1-mNeonGreen was generated by ligating a BglII-HindIII fragment containing a pRS305 backbone and the *GIC1* gene (from pDLB4401 = pRS305-GIC1-mScarlett) with a BamHI-HindIII digested PCR fragment containing mNeonGreen (from pDLB4393 = pRS305-BEM1-mNeonGreen). The resulting plasmid was digested with SphI to target integration at *GIC1*.

In cases where strain construction required mating of *ste20Δ* haploids, the strains were transformed with pDLB2677 (CEN STE20) to enable mating, and the diploid was then streaked to allow plasmid loss, and colonies that had lost the plasmid were selected.

Cell culture and cell cycle synchronization

Complete synthetic media (CSM; MP Biomedicals) with 2% dextrose (dex) was used to culture yeast cells to mid-log phase ($\sim 10^7$ /ml) at 30°C except for temperature-sensitive strains, which were cultured at 24°C. For live-cell imaging, cells were treated with 0.2 M hydroxyurea (HU; Sigma-Aldrich) for 3 h at 30°C or 4 h at 24°C, washed, released into fresh CSM + dex, and allowed to recover for 1 h at 30°C or 2 h at 24°C before imaging.

For Western blotting, cells were arrested in G1 by treatment with 2 μ M α -factor (GenWay Biotech) for 3 h, washed, and released into fresh CSM + dex. 15 μ g/ml nocodazole (Sigma-Aldrich) was added 1 h after release to block cells in mitosis, yielding a single cycle from G1 to M. Samples were taken, and budding percentage was scored at 15 min intervals. For determination of budding percentage, cells were fixed with 3.7% formaldehyde. At least 500 cells were scored for each sample.

Microscopy and image analysis

Cells were mounted onto 2% agarose (Denville Scientific) slabs with CSM + dex media. For the anchor away experiments, slabs were adjusted to 50 μ g/ml rapamycin (or DMSO for controls). Slab edges were sealed with petroleum jelly. Time-lapse videos were acquired at 30°C (or 24°C and 37°C as indicated for temperature-sensitive experiments) with an Andor Revolution XD spinning-disk confocal microscope (Olympus) with Andor Ixon3 897 512 electron-multiplying charge-coupled device (EMCCD) camera using MetaMorph software (Universal Imaging). A 100 \times /1.4 UplanSApo oil-immersion objective was used. Images (stacks of either 17 or 30 z-planes with 0.50- or 0.24- μ m spacing, respectively) were captured at 45-s intervals (for HU synchronized cells) or 90-s intervals (for asynchronous cells), using a 100-ms exposure and 200 gain on the EMCCD camera. Images were deconvolved with Huygens Essential software (Scientific Volume Imaging).

Image analysis was performed using a custom Matlab-based graphical user interface (GUI; ROI_TOI_QuantV8 [Lai et al.,

2018]). The GUI was used to calculate the CV of pixel intensities within a manually defined elliptical region circumscribing each cell on a maximum projection of the z-stack. The region was set to encompass the entire cell body with minimal noncell background at selected time frames and automatically interpolated in between, so that the region closely follows the cell shape and position over time. Fluorescence signal at the bud neck during and after cytokinesis was carefully excluded. The raw CV data were smoothed by spline fit (smooth window 10). The time of Whi5 50% nuclear exit was determined by interpolating the time when CV decreased to half of its peak value. For polarity proteins, the second derivative curve of the smoothed CV data was calculated. The time of polarization was called by the time when the second derivative curve reached a maximum. Occasionally, the highest CV peak did not correspond to the right time of the cell cycle, and the CV peak closest to the visually obvious onset of polarization was called.

Image analysis in Fig. S1 (B, D, and F) was performed using another Matlab-based GUI (NucTrackV3.3). The GUI used a threshold given by the standard Otsu algorithm to identify the nuclear Htb2 signal, and then the sum fluorescence intensity of Whi5 within the thresholded area was calculated and normalized to the peak intensity across the entire movie. Images of representative cells were generated using ImageJ (Fiji; National Institutes of Health). Image z-stacks were compiled to single plane by maximum projection, scaled, and inverted.

Statistical analysis

P values were calculated via a two-tailed *t* test for the null hypothesis that mothers and daughters of the same strain exhibit the same mean timing of polarization relative to either start or cytokinesis. Two asterisks denote a difference at $P < 0.01$, and three asterisks denote a difference at $P < 0.001$. We note that the differences between mother cells and prestart daughter cells discussed in the text were always large and significant at $P < 0.001$. Small differences between mother cells and poststart daughter cells were sometimes significant, but only at $P < 0.01$. These small differences are consistent with the conclusion that mothers and daughters have intrinsically different propensities to polarize.

Western blotting

Samples were prepared using TCA (Kozubowski et al., 2008) from $\sim 1 \times 10^7$ cells. Cells were collected and resuspended in pronase buffer (25 mM Tris-HCl, pH 7.5, 1.4 M Sorbitol, 20 mM Na₃N, and 2 mM MgCl₂). TCA (Sigma-Aldrich) was added to a final concentration of 17% wt/vol, and pellets were stored at -80°C . Cells were thawed and homogenized by vortexing with glass beads at 4°C for 10 min. Precipitated proteins were collected from lysates by centrifugation at 4°C and resuspended in sample buffer (40 mM Tris-HCl, pH 6.8, 8 M Urea, 5% SDS, 143 mM β -mercaptoethanol, 0.1 mM EDTA, and 0.4 mg/ml bromophenol blue), and the pH was titrated using 2 M Tris-HCl, pH 8.0. After SDS-PAGE and transfer, blots were probed using monoclonal mouse anti-GFP and anti-HA antibodies (Roche) at 1:1,000 dilution and anti-Cdc11 antibody (Santa Cruz Biotechnology) at 1:10,000 dilution. Fluorophore-conjugated secondary antibodies for mouse (IRDye800-conjugated goat anti-mouse

IgG; Rockland Immunochemicals) or rabbit (Alexa Fluor 680 goat anti-rabbit IgG; Invitrogen) were used at 1:5,000 dilution. Western blots were visualized using the ODYSSEY imaging system (LI-COR Biosciences).

Computational modeling

The models in this study were based on those published in Kuo et al. (2014) and Wu et al. (2015) comprising systems of reaction-diffusion equations. In the models, Cdc42 exists at the membrane in both its GDP-bound (Cdc42D_m) and GTP-bound (Cdc42T) forms. GDP-Cdc42 can exchange between the membrane (Cdc42D_m) and the cytoplasm (Cdc42D_c) through the action of the GDI. The action of the GDI is represented implicitly by first-order reactions with rate constants k_{5a} and k_{5b} . At the membrane, GDP/GTP exchange is catalyzed by the GEF with mass action kinetics (rate constants k_{2a} and k_3). GTP hydrolysis is catalyzed by GAPs, which are represented implicitly by a first-order reaction with rate k_{2b} . The GEF is in complex with Bem1 and PAK, denoted BemGEF, which exchanges between the membrane (BemGEF_m) and the cytoplasm (BemGEF_c) via first-order reactions with rate constants k_{1a} and k_{1b} . BemGEF complexes can bind GTP-Cdc42 at the membrane to yield BemGEF42 (association rate constants k_{4a} and k_7 and dissociation rate constant k_{4b}). Positive feedback arises because BemGEF interaction with GTP-Cdc42 leads to local enrichment of the GEF at sites with high GTP-Cdc42, generating more local GTP-Cdc42.

Whereas both models have positive feedback as outlined above, one model has additional negative feedback owing to inhibitory GEF phosphorylation by the PAK (Kuo et al., 2014). Phosphorylated GEF species are denoted by an asterisk: BemGEF_c^{*}, BemGEF_m^{*}, and BemGEF42^{*}. Phosphorylation is assumed to occur when the PAK in one BemGEF42 complex phosphorylates the GEF in another BemGEF42 complex at the membrane, modeled by mass action with rate constant k_8 . Dephosphorylation is assumed to occur in the cytoplasm, modeled as a first-order reaction with rate constant k_9 . Phosphorylated species are assumed to bind and dissociate from GTP-Cdc42 or the membrane at the same rates as dephosphorylated species, but they do not catalyze GTP-loading of Cdc42.

Diffusion of all membrane species is assumed to occur with diffusion constant D_m on a 2D discretized membrane of area equal to the surface of a 5-μm diameter sphere, with periodic boundary conditions. The “volume” of the membrane is 1% of the volume of the cytoplasm (accounted for by the factor η in model equations). In effect, the membrane is treated as a 10-nm-thick shell surrounding the cytoplasm. Diffusion in the cytoplasm is assumed to be fast enough (given the small size of yeast cells) that cytoplasmic species are well mixed. Almost all of the equations are deterministic; however, the concentration of the BemGEF complex at the membrane and in the cytoplasm is subject to Gaussian noise. noise Parameter values are given in Table S2. Simulations were performed using Matlab, and codes are available upon request.

Changes in the strength of positive feedback were modeled by altering k_7 , which controls the association of BemGEF_c with Cdc42T. Changes in the amount of GAP activity were modeled by altering k_{2b} . To model Rsr1, a spatially restricted Rsr1-GEF was

added to a 0.7-μm-diameter circle, providing a local basal level of GEF activity approximately equal to 1% of the GEF activity in a polarized Cdc42 peak.

Model equations

Positive feedback only

$$\begin{aligned}\frac{\partial \text{Cdc42T}}{\partial t} &= (k_r + k_{2a} \text{BemGEF}_m + k_3 \text{BemGEF42}) \times \text{Cdc42D}_m - \\ &\quad (k_{2b} + k_{4a} \text{BemGEF}_m + k_7 \text{BemGEF}_c) \times \text{Cdc42T} + k_{4b} \text{BemGEF42} \\ \frac{\partial \text{Cdc42D}_m}{\partial t} &= k_{2b} \text{Cdc42T} - (k_{2a} \text{BemGEF}_m + k_3 \text{BemGEF42}) \times \\ &\quad \text{Cdc42D}_m - k_{5b} \text{Cdc42D}_m + k_{5a} \text{Cdc42D}_c \\ \frac{\partial \text{Cdc42D}_c}{\partial t} &= \eta (k_{5b} \text{Cdc42D}_m - k_{5a} \text{Cdc42D}_c) \\ \frac{\partial \text{BemGEF42}}{\partial t} &= (k_{4a} \text{BemGEF}_m + k_7 \text{BemGEF}_c) \\ &\quad \times \text{Cdc42T} - k_{4b} \text{BemGEF42} \\ \frac{\partial \text{BemGEF}_m}{\partial t} &= k_{1a} \text{BemGEF}_c + k_{4b} \text{BemGEF42} - \\ &\quad (k_{1b} - k_{4a} \text{Cdc42T}) \times \text{BemGEF}_m - \sqrt{s} \xi(t) \\ \frac{\partial \text{BemGEF}_c}{\partial t} &= \eta [k_{1b} \text{BemGEF}_m - (k_{1a} + k_7 \text{Cdc42T}) \times \text{BemGEF}_c + \sqrt{s} \xi(t)]\end{aligned}$$

Positive and negative feedback

$$\begin{aligned}\frac{\partial \text{Cdc42T}}{\partial t} &= (k_r + k_{2a} \text{BemGEF}_m + k_3 \text{BemGEF42}) \times \\ &\quad \text{Cdc42D}_m - \left[k_{2b} + k_{4a} (\text{BemGEF}_m + \text{BemGEF}_m^*) + \right. \\ &\quad \left. k_7 (\text{BemGEF}_c + \text{BemGEF}_c^*) \right] \times \\ &\quad \text{Cdc42T} + k_{4b} (\text{BemGEF42} + \text{BemGEF42}^*) \\ \frac{\partial \text{Cdc42D}_m}{\partial t} &= k_{2b} \text{Cdc42T} - (k_{5b} + k_{2a} \text{BemGEF}_m + k_3 \text{BemGEF42}) \times \\ &\quad \text{Cdc42D}_m + k_{5a} \text{Cdc42D}_c \\ \frac{\partial \text{Cdc42D}_c}{\partial t} &= \eta (k_{5b} \text{Cdc42D}_m - k_{5a} \text{Cdc42D}_c) \\ \frac{\partial \text{BemGEF42}}{\partial t} &= (k_{4a} \text{BemGEF}_m + k_7 \text{BemGEF}_c) \times \text{Cdc42T} - \\ &\quad [k_{4b} + k_8 (\text{BemGEF42} + \text{BemGEF42}^*)] \times \text{BemGEF42} \\ \frac{\partial \text{BemGEF42}^*}{\partial t} &= (k_{4a} \text{BemGEF}_m^* + k_7 \text{BemGEF}_c^*) \times \text{Cdc42T} - \\ &\quad k_{4b} \text{BemGEF42}^* + k_8 (\text{BemGEF42} + \text{BemGEF42}^*) \times \text{BemGEF42} \\ \frac{\partial \text{BemGEF}_m}{\partial t} &= k_{1a} \text{BemGEF}_c + k_{4b} \text{BemGEF42} - \\ &\quad (k_{1b} + k_{4a} \text{Cdc42T}) \times \text{BemGEF}_m - \sqrt{s} \xi(t) \\ \frac{\partial \text{BemGEF}_m^*}{\partial t} &= k_{1a} \text{BemGEF}_c^* + k_{4b} \text{BemGEF42}^* - (k_{1b} + k_{4a} \text{Cdc42T}) \\ &\quad \times \text{BemGEF}_m^* \\ \frac{\partial \text{BemGEF}_c}{\partial t} &= \eta \left[k_{1b} \text{BemGEF}_m - (k_{1a} + k_7 \text{Cdc42T}) \times \right. \\ &\quad \left. \text{BemGEF}_c + \sqrt{s} \xi(t) \right] + k_9 \text{BemGEF}_c^* \\ \frac{\partial \text{BemGEF}_c^*}{\partial t} &= \eta [k_{1b} \text{BemGEF}_m^* - (k_{1a} + k_7 \text{Cdc42T}) \times \text{BemGEF}_c^*] - \\ &\quad k_9 \text{BemGEF}_c^*\end{aligned}$$

where

$$k_8 = k_{8\max} \frac{(BemGEF42 + BemGEF42^*)^{k_{8n}}}{k_{8h}^{k_{8n}} + (BemGEF42 + BemGEF42^*)^{k_{8n}}}$$

$$k_9 = k_{9\max} \frac{(BemGEF_c^*)^{k_{9n}}}{k_{9h}^{k_{9n}} + (BemGEF_c^*)^{k_{9n}}}$$

Online supplemental material

Fig. S1 shows control experiments to validate the strategy for determining the time of start. Fig. S2 shows control experiments to validate the strategy for determining the time of polarization. Fig. S3 shows that haploid cells display a similar timing of polarization relative to start as the diploid cells shown in Fig. 1. Table S1 lists the yeast strains used in this study. Table S2 lists the model parameters used in this study.

Acknowledgments

Thanks to H. Chen for the motivation to reinvestigate the role of cell cycle in polarity control. We thank N. Buchler, S. Di Talia, S. Haase, A. Gladfelter, T. Elston, and members of the D.J.L. laboratory for thoughtful discussions and critical readings of the manuscript. Thanks to J. Skotheim (Stanford University) and P. Pryciak (University of Massachusetts) for yeast strains and plasmids.

This work was funded by National Institute of General Medical Sciences, National Institutes of Health grants GM62300 and GM122488 to D.J. Lew and by Army Research Office grant W911NF-17-1-0395 to D. Tsygankov.

The authors declare no competing financial interests.

Author contributions: K.D. Moran, H. Kang, and D.J. Lew designed and analyzed experiments; K.D. Moran, H. Kang, K. Saito, and A.V. Araujo performed experiments; D. Tsygankov generated image analysis tools, T.R. Zyla generated plasmids and yeast strains; and K.D. Moran, H. Kang, and D.J. Lew wrote and edited the paper.

Submitted: 27 June 2018

Revised: 21 September 2018

Accepted: 18 October 2018

References

- Atkins, B.D., S. Yoshida, K. Saito, C.F. Wu, D.J. Lew, and D. Pellman. 2013. Inhibition of Cdc42 during mitotic exit is required for cytokinesis. *J. Cell Biol.* 202:231–240. <https://doi.org/10.1083/jcb.201301090>
- Bi, E., and H.O. Park. 2012. Cell polarization and cytokinesis in budding yeast. *Genetics*. 191:347–387. <https://doi.org/10.1534/genetics.111.132886>
- Bobola, N., R.P. Jansen, T.H. Shin, and K. Nasmyth. 1996. Asymmetric accumulation of Ash1p in postanaphase nuclei depends on a myosin and restricts yeast mating-type switching to mother cells. *Cell*. 84:699–709. [https://doi.org/10.1016/S0092-8674\(00\)81048-X](https://doi.org/10.1016/S0092-8674(00)81048-X)
- Bose, I., J.E. Irazoqui, J.J. Moskow, E.S. Bardes, T.R. Zyla, and D.J. Lew. 2001. Assembly of scaffold-mediated complexes containing Cdc42p, the exchange factor Cdc24p, and the effector Cla4p required for cell cycle-regulated phosphorylation of Cdc24p. *J. Biol. Chem.* 276:7176–7186. <https://doi.org/10.1074/jbc.M010546200>
- Brown, J.L., M. Jaquenoud, M.P. Gulli, J. Chant, and M. Peter. 1997. Novel Cdc42-binding proteins Gic1 and Gic2 control cell polarity in yeast. *Genes Dev.* 11:2972–2982. <https://doi.org/10.1101/gad.11.22.2972>

- Butty, A.C., N. Perrinjaquet, A. Petit, M. Jaquenoud, J.E. Segall, K. Hofmann, C. Zwahlen, and M. Peter. 2002. A positive feedback loop stabilizes the guanine-nucleotide exchange factor Cdc24 at sites of polarization. *EMBO J.* 21:1565–1576. <https://doi.org/10.1093/emboj/21.7.1565>
- Caviston, J.P., M. Longtine, J.R. Pringle, and E. Bi. 2003. The role of Cdc42p GTPase-activating proteins in assembly of the septin ring in yeast. *Mol. Biol. Cell*. 14:4051–4066. <https://doi.org/10.1091/mbc.e03-04-0247>
- Chant, J. 1999. Cell polarity in yeast. *Annu. Rev. Cell Dev. Biol.* 15:365–391. <https://doi.org/10.1146/annurev.cellbio.15.1.365>
- Chen, G.C., Y.J. Kim, and C.S. Chan. 1997. The Cdc42 GTPase-associated proteins Gic1 and Gic2 are required for polarized cell growth in *Saccharomyces cerevisiae*. *Genes Dev.* 11:2958–2971. <https://doi.org/10.1101/gad.11.22.2958>
- Chen, H., C.C. Kuo, H. Kang, A.S. Howell, T.R. Zyla, M. Jin, and D.J. Lew. 2012. Cdc42p regulation of the yeast formin Bni1p mediated by the effector Gic2p. *Mol. Biol. Cell*. 23:3814–3826. <https://doi.org/10.1091/mbc.e12-05-0400>
- Colman-Lerner, A., T.E. Chin, and R. Brent. 2001. Yeast Cbk1 and Mob2 activate daughter-specific genetic programs to induce asymmetric cell fates. *Cell*. 107:739–750. [https://doi.org/10.1016/S0092-8674\(01\)00596-7](https://doi.org/10.1016/S0092-8674(01)00596-7)
- Costanzo, M., J.L. Nishikawa, X. Tang, J.S. Millman, O. Schub, K. Breitkreuz, D. Dewar, I. Rupes, B. Andrews, and M. Tyers. 2004. CDK activity antagonizes Whi5, an inhibitor of G1/S transcription in yeast. *Cell*. 117:899–913. <https://doi.org/10.1016/j.cell.2004.05.024>
- de Bruin, R.A., W.H. McDonald, T.I. Kalashnikova, J. Yates III, and C. Wittenberg. 2004. Cln3 activates G1-specific transcription via phosphorylation of the SBF bound repressor Whi5. *Cell*. 117:887–898. <https://doi.org/10.1016/j.cell.2004.05.025>
- Di Talia, S., J.M. Skotheim, J.M. Bean, E.D. Siggia, and F.R. Cross. 2007. The effects of molecular noise and size control on variability in the budding yeast cell cycle. *Nature*. 448:947–951. <https://doi.org/10.1038/nature06072>
- Di Talia, S., H. Wang, J.M. Skotheim, A.P. Rosebrock, B. Fletcher, and F.R. Cross. 2009. Daughter-specific transcription factors regulate cell size control in budding yeast. *PLoS Biol.* 7:e1000221. <https://doi.org/10.1371/journal.pbio.1000221>
- Doncic, A., M. Faller-Fettig, and J.M. Skotheim. 2011. Distinct interactions select and maintain a specific cell fate. *Mol. Cell*. 43:528–539. <https://doi.org/10.1016/j.molcel.2011.06.025>
- Evangelista, M., K. Blundell, M.S. Longtine, C.J. Chow, N. Adames, J.R. Pringle, M. Peter, and C. Boone. 1997. Bni1p, a yeast formin linking Cdc42p and the actin cytoskeleton during polarized morphogenesis. *Science*. 276:118–122. <https://doi.org/10.1126/science.276.5309.118>
- Gao, X.D., L.M. Sperber, S.A. Kane, Z. Tong, A.H. Tong, C. Boone, and E. Bi. 2007. Sequential and distinct roles of the cadherin domain-containing protein Axl2p in cell polarization in yeast cell cycle. *Mol. Biol. Cell*. 18:2542–2560. <https://doi.org/10.1091/mbc.e06-09-0822>
- Gladfelter, A.S., J.J. Moskow, T.R. Zyla, and D.J. Lew. 2001. Isolation and characterization of effector-loop mutants of CDC42 in yeast. *Mol. Biol. Cell*. 12:1239–1255. <https://doi.org/10.1091/mbc.12.5.1239>
- Goryachev, A.B., and A.V. Pokhilko. 2008. Dynamics of Cdc42 network embodies a Turing-type mechanism of yeast cell polarity. *FEBS Lett.* 582:1437–1443. <https://doi.org/10.1016/j.febslet.2008.03.029>
- Gulli, M.P., M. Jaquenoud, Y. Shimada, G. Niederhäuser, P. Wiget, and M. Peter. 2000. Phosphorylation of the Cdc42 exchange factor Cdc24 by the PAK-like kinase Cla4 may regulate polarized growth in yeast. *Mol. Cell*. 6:1155–1167. [https://doi.org/10.1016/S1097-2765\(00\)00113-1](https://doi.org/10.1016/S1097-2765(00)00113-1)
- Han, B.K., L.M. Bogomolnaya, J.M. Totten, H.M. Blank, L.J. Dangott, and M. Polymenis. 2005. Bem1p, a scaffold signaling protein, mediates cyclin-dependent control of vacuolar homeostasis in *Saccharomyces cerevisiae*. *Genes Dev.* 19:2606–2618. <https://doi.org/10.1101/gad.1361505>
- Harkins, H.A., N. Pagé, L.R. Schenkman, C. De Virgilio, S. Shaw, H. Bussey, and J.R. Pringle. 2001. Bud8p and Bud9p, proteins that may mark the sites for bipolar budding in yeast. *Mol. Biol. Cell*. 12:2497–2518. <https://doi.org/10.1091/mbc.12.8.2497>
- Haruki, H., J. Nishikawa, and U.K. Laemmli. 2008. The anchor-away technique: rapid, conditional establishment of yeast mutant phenotypes. *Mol. Cell*. 31:925–932. <https://doi.org/10.1016/j.molcel.2008.07.020>
- Howell, A.S., and D.J. Lew. 2012. Morphogenesis and the cell cycle. *Genetics*. 190:51–77. <https://doi.org/10.1534/genetics.111.128314>
- Howell, A.S., N.S. Savage, S.A. Johnson, I. Bose, A.W. Wagner, T.R. Zyla, H.F. Nijhout, M.C. Reed, A.B. Goryachev, and D.J. Lew. 2009. Singularity in

- polarization: rewiring yeast cells to make two buds. *Cell*. 139:731–743. <https://doi.org/10.1016/j.cell.2009.10.024>
- Howell, A.S., M. Jin, C.F. Wu, T.R. Zyla, T.C. Elston, and D.J. Lew. 2012. Negative feedback enhances robustness in the yeast polarity establishment circuit. *Cell*. 149:322–333. <https://doi.org/10.1016/j.cell.2012.03.012>
- Irazoqui, J.E., A.S. Gladfelter, and D.J. Lew. 2003. Scaffold-mediated symmetry breaking by Cdc42p. *Nat. Cell Biol.* 5:1062–1070. <https://doi.org/10.1038/ncb1068>
- Jansen, R.P., C. Dowzer, C. Michaelis, M. Galova, and K. Nasmyth. 1996. Mother cell-specific HO expression in budding yeast depends on the unconventional myosin myo4p and other cytoplasmic proteins. *Cell*. 84:687–697. [https://doi.org/10.1016/S0092-8674\(00\)81047-8](https://doi.org/10.1016/S0092-8674(00)81047-8)
- Jaquenoud, M., and M. Peter. 2000. Gic2p may link activated Cdc42p to components involved in actin polarization, including Bni1p and Bud6p (Aip3p). *Mol. Cell Biol.* 20:6244–6258. <https://doi.org/10.1128/MCB.20.17.6244-6258.2000>
- Johnson, J.M., M. Jin, and D.J. Lew. 2011. Symmetry breaking and the establishment of cell polarity in budding yeast. *Curr. Opin. Genet. Dev.* 21:740–746. <https://doi.org/10.1016/j.gde.2011.09.007>
- Johnston, G.C., J.P. Pringle, and L.H. Hartwell. 1977. Coordination of growth with cell division in the yeast *S. cerevisiae*. *Exp. Cell Res.* 105:79–98. [https://doi.org/10.1016/0014-4827\(77\)90154-9](https://doi.org/10.1016/0014-4827(77)90154-9)
- Jost, A.P., and O.D. Weiner. 2015. Probing Yeast Polarity with Acute, Reversible, Optogenetic Inhibition of Protein Function. *ACS Synth. Biol.* 4:1077–1085. <https://doi.org/10.1021/acssynbio.5b00053>
- Kang, P.J., M.E. Lee, and H.O. Park. 2014. Bud3 activates Cdc42 to establish a proper growth site in budding yeast. *J. Cell Biol.* 206:19–28. <https://doi.org/10.1083/jcb.201402040>
- Knaus, M., M.P. Pelli-Gulli, F. van Drogen, S. Springer, M. Jaquenoud, and M. Peter. 2007. Phosphorylation of Bem2p and Bem3p may contribute to local activation of Cdc42p at bud emergence. *EMBO J.* 26:4501–4513. <https://doi.org/10.1038/sj.emboj.7601873>
- Kozminski, K.G., L. Beven, E. Angerman, A.H. Tong, C. Boone, and H.O. Park. 2003. Interaction between a Ras and a Rho GTPase couples selection of a growth site to the development of cell polarity in yeast. *Mol. Biol. Cell*. 14:4958–4970. <https://doi.org/10.1091/mbc.e03-06-0426>
- Kozubowski, L., K. Saito, J.M. Johnson, A.S. Howell, T.R. Zyla, and D.J. Lew. 2008. Symmetry-breaking polarization driven by a Cdc42p GEF-PAK complex. *Curr. Biol.* 18:1719–1726. <https://doi.org/10.1016/j.cub.2008.09.060>
- Kuo, C.C., N.S. Savage, H. Chen, C.F. Wu, T.R. Zyla, and D.J. Lew. 2014. Inhibitory GEF phosphorylation provides negative feedback in the yeast polarity circuit. *Curr. Biol.* 24:753–759. <https://doi.org/10.1016/j.cub.2014.02.024>
- Lai, H., J.G. Chiou, A. Zhurikhina, T.R. Zyla, D. Tsygankov, and D.J. Lew. 2018. Temporal regulation of morphogenetic events in *Saccharomyces cerevisiae*. *Mol. Biol. Cell*. 29:2069–2083. <https://doi.org/10.1091/mbc.E18-03-0188>
- Lamson, R.E., M.J. Winters, and P.M. Pryciak. 2002. Cdc42 regulation of kinase activity and signaling by the yeast p21-activated kinase Ste20. *Mol. Cell Biol.* 22:2939–2951. <https://doi.org/10.1128/MCB.22.9.2939-2951.2002>
- Leberer, E., D. Dignard, D. Marcus, D.Y. Thomas, and M. Whiteway. 1992. The protein kinase homologue Ste20p is required to link the yeast pheromone response G-protein beta gamma subunits to downstream signaling components. *EMBO J.* 11:4815–4824. <https://doi.org/10.1002/j.1460-2075.1992.tb05587.x>
- Leberer, E., D.Y. Thomas, and M. Whiteway. 1997. Pheromone signalling and polarized morphogenesis in yeast. *Curr. Opin. Genet. Dev.* 7:59–66. [https://doi.org/10.1016/S0959-437X\(97\)80110-4](https://doi.org/10.1016/S0959-437X(97)80110-4)
- Lee, M.E., W.C. Lo, K.E. Miller, C.S. Chou, and H.O. Park. 2015. Regulation of Cdc42 polarization by the Rsr1 GTPase and Rga1, a Cdc42 GTPase-activating protein, in budding yeast. *J. Cell Sci.* 128:2106–2117. <https://doi.org/10.1242/jcs.166538>
- Lew, D.J., and S.I. Reed. 1993. Morphogenesis in the yeast cell cycle: regulation by Cdc28 and cyclins. *J. Cell Biol.* 120:1305–1320. <https://doi.org/10.1083/jcb.120.6.1305>
- Longtine, M.S., A. McKenzie III, D.J. Demarini, N.G. Shah, A. Wach, A. Brachat, P. Philippson, and J.R. Pringle. 1998. Additional modules for versatile and economical PCR-based gene deletion and modification in *Saccharomyces cerevisiae*. *Yeast*. 14:953–961. [https://doi.org/10.1002/\(SICI\)1097-0061\(199807\)14:10%3C953::AID-YEA293%3E3.0.CO;2-U](https://doi.org/10.1002/(SICI)1097-0061(199807)14:10%3C953::AID-YEA293%3E3.0.CO;2-U)
- McCusker, D., C. Denison, S. Anderson, T.A. Egelhofer, J.R. Yates III, S.P. Gygi, and D.R. Kellogg. 2007. Cdk1 coordinates cell-surface growth with the cell cycle. *Nat. Cell Biol.* 9:506–515. <https://doi.org/10.1038/ncb1568>
- Morgan, D.O. 1997. Cyclin-dependent kinases: engines, clocks, and microprocessors. *Annu. Rev. Cell Dev. Biol.* 13:261–291. <https://doi.org/10.1146/annurev.cellbio.13.1.261>
- Mösch, H.U., R.L. Roberts, and G.R. Fink. 1996. Ras2 signals via the Cdc42/Ste20/mitogen-activated protein kinase module to induce filamentous growth in *Saccharomyces cerevisiae*. *Proc. Natl. Acad. Sci. USA*. 93:5352–5356. <https://doi.org/10.1073/pnas.93.11.5352>
- Moskow, J.J., A.S. Gladfelter, R.E. Lamson, P.M. Pryciak, and D.J. Lew. 2000. Role of Cdc42p in pheromone-stimulated signal transduction in *Saccharomyces cerevisiae*. *Mol. Cell Biol.* 20:7559–7571. <https://doi.org/10.1128/MCB.20.20.7559-7571.2000>
- Nelson, B., C. Kurischko, J. Horecka, M. Mody, P. Nair, L. Pratt, A. Zougman, L.D. McBroom, T.R. Hughes, C. Boone, and F.C. Luca. 2003. RAM: a conserved signaling network that regulates Ace2p transcriptional activity and polarized morphogenesis. *Mol. Biol. Cell*. 14:3782–3803. <https://doi.org/10.1091/mbc.e03-01-0018>
- Oda, Y., K. Huang, F.R. Cross, D. Cowburn, and B.T. Chait. 1999. Accurate quantitation of protein expression and site-specific phosphorylation. *Proc. Natl. Acad. Sci. USA*. 96:6591–6596. <https://doi.org/10.1073/pnas.96.12.6591>
- Onishi, M., N. Ko, R. Nishihama, and J.R. Pringle. 2013. Distinct roles of Rho1, Cdc42, and Cyk3 in septum formation and abscission during yeast cytokinesis. *J. Cell Biol.* 202:311–329. <https://doi.org/10.1083/jcb.201302001>
- Padmashree, C.G., and U. Surana. 2001. Cdc28-Clb mitotic kinase negatively regulates bud site assembly in the budding yeast. *J. Cell Sci.* 114:207–218.
- Park, H.O., and E. Bi. 2007. Central roles of small GTPases in the development of cell polarity in yeast and beyond. *Microbiol. Mol. Biol. Rev.* 71:48–96. <https://doi.org/10.1128/MMBR.00028-06>
- Pringle, J.R., and L.H. Hartwell. 1981. The *Saccharomyces cerevisiae* cell cycle. In *The Molecular Biology of the Yeast Saccharomyces*. J.D. Strathern, E.W. Jones, and J.R. Broach, editors. Cold Spring Harbor Laboratory, Cold Spring Harbor, N.Y. 97–142.
- Sheu, Y.J., Y. Barral, and M. Snyder. 2000. Polarized growth controls cell shape and bipolar bud site selection in *Saccharomyces cerevisiae*. *Mol. Cell Biol.* 20:5235–5247. <https://doi.org/10.1128/MCB.20.14.5235-5247.2000>
- Shimada, Y., P. Wiget, M.P. Gulli, E. Bi, and M. Peter. 2004. The nucleotide exchange factor Cdc24p may be regulated by auto-inhibition. *EMBO J.* 23:1051–1062. <https://doi.org/10.1038/sj.emboj.7600124>
- Sil, A., and I. Herskowitz. 1996. Identification of asymmetrically localized determinant, Ash1p, required for lineage-specific transcription of the yeast HO gene. *Cell*. 84:711–722. [https://doi.org/10.1016/S0092-8674\(00\)81049-1](https://doi.org/10.1016/S0092-8674(00)81049-1)
- Skotheim, J.M., S. Di Talia, E.D. Siggia, and F.R. Cross. 2008. Positive feedback of G1 cyclins ensures coherent cell cycle entry. *Nature*. 454:291–296. <https://doi.org/10.1038/nature07118>
- Sloat, B.F., A. Adams, and J.R. Pringle. 1981. Roles of the *CDC24* gene product in cellular morphogenesis during the *Saccharomyces cerevisiae* cell cycle. *J. Cell Biol.* 89:395–405. <https://doi.org/10.1083/jcb.89.3.395>
- Sopko, R., D. Huang, J.C. Smith, D. Figeys, and B.J. Andrews. 2007. Activation of the Cdc42p GTPase by cyclin-dependent protein kinases in budding yeast. *EMBO J.* 26:4487–4500. <https://doi.org/10.1038/sj.emboj.7601847>
- Takahashi, S., and P.M. Pryciak. 2007. Identification of novel membrane-binding domains in multiple yeast Cdc42 effectors. *Mol. Biol. Cell*. 18:4945–4956. <https://doi.org/10.1091/mbc.e07-07-0676>
- Wai, S.C., S.A. Gerber, and R. Li. 2009. Multisite phosphorylation of the guanine nucleotide exchange factor Cdc24 during yeast cell polarization. *PLoS One*. 4:e6563. <https://doi.org/10.1371/journal.pone.0006563>
- Wedlich-Soldner, R., S.C. Wai, T. Schmidt, and R. Li. 2004. Robust cell polarity is a dynamic state established by coupling transport and GTPase signaling. *J. Cell Biol.* 166:889–900. <https://doi.org/10.1083/jcb.200405061>
- Weiss, E.L., A.C. Bishop, K.M. Shokat, and D.G. Drubin. 2000. Chemical genetic analysis of the budding-yeast p21-activated kinase Cla4p. *Nat. Cell Biol.* 2:677–685. <https://doi.org/10.1038/35036300>
- Wild, A.C., J.W. Yu, M.A. Lemmon, and K.J. Blumer. 2004. The p21-activated protein kinase-related kinase Cla4 is a coincidence detector of signaling by Cdc42 and phosphatidylinositol 4-phosphate. *J. Biol. Chem.* 279:17101–17110. <https://doi.org/10.1074/jbc.M314035200>
- Winters, M.J., and P.M. Pryciak. 2005. Interaction with the SH3 domain protein Bem1 regulates signaling by the *Saccharomyces cerevisiae* p21-activated kinase Ste20. *Mol. Cell Biol.* 25:2177–2190. <https://doi.org/10.1128/MCB.25.6.2177-2190.2005>
- Witte, K., D. Strickland, and M. Glotzer. 2017. Cell cycle entry triggers a switch between two modes of Cdc42 activation during yeast polarization. *eLife*. 6:e26722. <https://doi.org/10.7554/eLife.26722>

- Woods, B., C.C. Kuo, C.F. Wu, T.R. Zyla, and D.J. Lew. 2015. Polarity establishment requires localized activation of Cdc42. *J. Cell Biol.* 211:19–26. <https://doi.org/10.1083/jcb.201506108>
- Woods, B., H. Lai, C.F. Wu, T.R. Zyla, N.S. Savage, and D.J. Lew. 2016. Parallel Actin-Independent Recycling Pathways Polarize Cdc42 in Budding Yeast. *Curr. Biol.* 26:2114–2126. <https://doi.org/10.1016/j.cub.2016.06.047>
- Wu, C.F., N.S. Savage, and D.J. Lew. 2013. Interaction between bud-site selection and polarity-establishment machineries in budding yeast. *Philos. Trans. R. Soc. Lond. B Biol. Sci.* 368:20130006. <https://doi.org/10.1098/rstb.2013.0006>
- Wu, C.F., J.G. Chiou, M. Minakova, B. Woods, D. Tsygankov, T.R. Zyla, N.S. Savage, T.C. Elston, and D.J. Lew. 2015. Role of competition between polarity sites in establishing a unique front. *eLife*. 4:e11611. <https://doi.org/10.7554/eLife.11611>
- Wu, H., C. Turner, J. Gardner, B. Temple, and P. Brennwald. 2010. The Exo70 subunit of the exocyst is an effector for both Cdc42 and Rho3 function in polarized exocytosis. *Mol. Biol. Cell.* 21:430–442. <https://doi.org/10.1091/mbc.e09-06-0501>
- Zheng, Y., A. Bender, and R.A. Cerione. 1995. Interactions among proteins involved in bud-site selection and bud-site assembly in *Saccharomyces cerevisiae*. *J. Biol. Chem.* 270:626–630. <https://doi.org/10.1074/jbc.270.2.626>
- Ziman, M., D. Preuss, J. Mulholland, J.M. O'Brien, D. Botstein, and D.I. Johnson. 1993. Subcellular localization of Cdc42p, a *Saccharomyces cerevisiae* GTP-binding protein involved in the control of cell polarity. *Mol. Biol. Cell.* 4:1307–1316. <https://doi.org/10.1091/mbc.4.12.1307>